

We are very grateful to the two reviewers for their helpful observations, comments, and suggestions.

In the following file, please find a point-by-point response to the reviews and the reviewed version of the manuscript with changes marked-up.

Referee #1

Interactive comment on “Composition and Vertical Flux of Particulate Organic Matter to the Oxygen Minimum Zone of the Central Baltic Sea: Impact of a sporadic North Sea inflow”

by Carolina Cisternas-Novoa

Anonymous Referee #1 Received and published: 19 September 2018

The authors demonstrate their investigations of particulate matter in the water column and in sediment traps in two basins (Gotland Basin (GB) and Landsort Deep (LD)) to estimate its composition and the particle flux in these basins and how it changes dependent if the deep water is oxygenated or not. Thus, the manuscript can be a significant contribution to understand the biogeochemical processes and its spatial variation in the Baltic Sea. However, the ms is difficult to read and to get a ‘take home message’ because it contains many nonspecific verbalization. For example, it is often unclear which depth horizons are meant or why the situation at a certain depth is mentioned at this place (e.g. 110m in line 31).

The influence of the MPI must be presented more clearly and substantiated. This requires comparison of a defined depth range which is oxygen rich in one basin and low in oxygen in the other. In the GB, the situation after MBI should be compared with a situation during a stagnation period, if possible. Many of these things are present in the ms but not clearly and focused demonstrated. I would expect from the title what is transported from the overlaying layers to the OMZ. Indeed, data for the whole water column of the GB and up to 200m in the LD are given without any Accentuations.

Abstract: The objectives are not clear Line 17-18: “Oxygen (O₂) depletion may improve the efficiency of the biological carbon pump”. Is this sentence the hypothesis of the work? If yes, than it has to be indicated and it needs to be answered at the end of the abstract.

AR: We will add information to the abstract, about the oxygen conditions at each depth where we deployed a sediment trap in GB and LD (ex: oxygenated surface, the core of the oxygen minimum zone and deep water oxygenated by the inflow) to clarify why we mention specific depths.

We explicitly add the hypothesis and rephrase the objectives for clarity. We answered the hypothesis at the end of the abstract when we expose the differences in POM and export between the two studied stations, and we propose a mechanism to explain those differences.

Information about oxygen conditions at depths where sediment traps were deployed in each station was added in L22-25. We explicitly add the hypothesis to the abstract (L25-27)

Line 20-21: I would replace “Major Baltic Inflow “by“ salt water inflow” here.

AR: This was change to “a major oxygen-rich saltwater inflow” (L21)

Line 24-32: It is difficult to understand what the comparison of the two depths means for the task.

AR: This paragraph was modified for clarity and as mentioned above, the oxygen conditions at each depth are mentioned (ex: oxygenated surface, the core of the oxygen minimum zone and deep water oxygenated by the inflow)

Line 29: Why “contrastingly”? POC and PN decreased too.

AR: We agree this was confusing “contrastingly” was deleted

Line 33: why “may form”? I think it is a result of this work.

AR: We said “may form” because, as we explain in the next line, our results suggest that MnOx-like particles aggregate with POM, this is what we propose. However, we think that to ensure that MnOx and POM aggregate and the specific composition of those aggregates, we will need to investigate aggregate formation and composition further.

Line 38: sink instead of sank

AR: This has been fixed.

Introduction:

Line 78-80: “. . .(Tamelander et al. 2017)”. Please replace “On the long term, a decrease in OM downward flux may limit the oxygen depletion.” By “The reduction of nutrient inputs as target by HELCOM can cause a decrease in OM downward flux and limit the oxygen depletion.”

AR: The sentence has been replaced according to the reviewer suggestion.

Line79-80. I would delete the last sentence of the chapter.

AR: The last sentence of the paragraph “However, to fully suppress hypoxia enhanced ventilation would be necessary the bottom waters of the Baltic Sea” is to emphasize that the bottom-water oxygen concentrations, are not only controlled by the nutrient loads, but also by physical factors like the frequency and intensity of the saltier water inflow, which had a decadal variability and it is modulated by meteorological forcing (e.g., Carstensen et al. 2014). This is explained in the next paragraph.

Line 88: “. . . Carstensen et al. 2014)”. Recommendation: Salt water inflows from the North Sea. . . .

AR: The sentence has been modified according to the reviewer recommendation.

Line 91-92 “Saltier, denser, O₂-rich North Sea waters entered the western Baltic Sea in December 2014 and reached the Gotland Basin on February 2015.” The sentence could be deleted.

Line 92-95: “At the time of sampling, this MBI also affected the neighboring Faroe Deep; but not the LD, located further northwest. The sentence can be deleted.

AR: We modified this paragraph and combined those sentences as “At the time of sampling, this MBI had reached the Gotland Basin, but did not affect the LD, located further northwest.” to emphasize that the MBI oxygenated the deep waters of GB, but not those of LD (L97-98).

Line 100: Please add the water depth in which the redox lines occur.

AR: We added the redoxcline depth from literature (between 120 and 150 m depth; L102). In the results, we define the redoxcline depth determined from the O₂ and H₂S concentrations during our sampling.

Line 99-100: This chapter can be shortened and combined with the chapter before.

AR: We think that provide background information on the chemical reactions occurring in the redoxcline, and how previous MBI had altered redox conditions, is important to frame our idea that changes in oxygenation enhance the formation of MnOx that aggregate with POM and alter POM distribution and export

Line 118-119: “enriched with OM; specifically with transparent exopolymer particles”.

AR: This has been fixed (L122).

Line 134-142: A clear objective is missing here.

AR: This paragraph has been modified to clarify the objectives of the study (L138-146)

Methods

Line 146: "surface-tethered sediment traps“that’s not true. Traps were also installed in 180 m

AR: As explained in the section “Sediment trap design and deployment”(L158-164) and in more detail in Engel et al. 2017 and Knauer et al. 1979, our traps consisted of 12 particle interceptor tubes (PITs) framed in five PVC crosses. Crosses with PITs tubes are attached at four depths: 2 at 40m, 60m, 110m, and 180m. The entire array is attached to the flotation gear that consists on a polypropylene line attached to two different types of flotation spheres. The entire flotation array is secured to the surface spar (a large yellow buoy) on which the flashlight and positioning systems are mounted.

Line 147-148: depth of water sampling should be given here.

AR: Water sampling depths are in table 2; this was added to the text (L152)

Line 150: conductivity temperature depth? Suggestion: Temperature, salinity and O₂ concentration were determined at each station using a Sea-Bird (CTD) probe equipped with a oxygen (Oxyguard, PreSens) sensor that was calibrated. . .

AR: This paragraph has been modified according to the reviewer recommendations (L153-154)

Line 155: According to Table 1, there are 3 or 4 depths in which the traps were exposed. That should be mentioned here as well.

AR: The sediment trap depths were added to the text (L158).

Line 174-178: Ammonium has to be measured in an unfiltered sample. However if samples for nutrient analysis are stored frozen and analyzed using an auto-analyzer, then filtration is necessary. Please correct.

AR: We thank the reviewer for this observation. The paragraph was corrected (L176-181).

Line 191-192: Please add the wave lengths

AR: The wavelengths were added to the text (440/685 nm; L195)

Line 215-219: Suggestion: "Particle number and area was measured semiautomatically using an image analysis system including the WCIF ImageJ software. Image analysis of TEP and CSP were and conducted after Engel (2009). Additionally, TEP and CSP in water samples from the stations where we deployed sediment traps were analysed spectrophotometrically according to Passow and Alldredge (1995) and Cisternas et al. (2014) respectively. Why was the additional method applied?"

AR: We modified the sentence according to the reviewer suggestion (L219-222). The additional spectrophotometrically method was used to measure TEP and CSP concentration in the water column. Since the spectrophotometric method is less labor intensive, it allows for sampling of the water column with higher vertical resolution (between 9 and 12 depths; L223)

Line 223: For TEP and CSP it should be mentioned that the red and the green channel were used?. Here should only be mentioned that the blue channel was used.

AR: We modified the TEP, CSP (L219-222) and MnOx (L230-232) image analysis section according to the reviewer suggestion.

Line 226 and line 233: Please delete the word "directly". When storing samples, there is no direct measurement.

AR: We deleted the word "directly"

Results Generally: I suggest that the results should be demonstrated for the basins successively (at first for the GB and after it for the LD) and not switched between the basins. In the vertical direction it should be started with the surface then successively the deeper layers whereby the depth of each layer should be defined to understand the results reported thereafter. Information about temperature and salinity is missing in the text.

Line 250-251: Information about the thermocline should be moved to the beginning of the chapter. The traps were exposed for one or two days. The water samples were taken at the same time. I don't believe that there was such a large range where the thermocline was located during this short time.

AR: The organization of this paragraph was changed according to the reviewer suggestion, i.e. Temperature, salinity and O₂ conditions were discussed first in GB and then in LD. Information about temperature and salinity were added to the text. We include the thermocline information

based on the measurements made during the deployment of the sediment traps. The depth range presented correspond to the initial and end depth were the temperature had a rapid decreased, this information was added to the text.

Line 259: Which depth is meant with surface water?

AR: We added to the text that surface water mean upper 10 m.

Line 260: Suggestion for changes: (6 μM at 80 and 140 m, and 0.12 260 μM at 110 m). It could be added already here that the upper (80m) and lower (140m) bounds and 110m the core of the OMZ are. It is mentioned later, but it should be already included here.

AR: We added the information about upper, lower oxycline and OMZ core in this sentence (L278-279).

Line 270: Because the conditions in water column are reported, it should be mentioned that nitrite had a maximum at 370m (Fig.2).

AR: We added the maximum of nitrite at 250 m and nitrate at 400 m to the text (L291-292)

Line 273-274: To which depth the second nutrient values apply; “the upper 110m” is confusing here.

Line 275: 0.22 μM ?

Line 269-276: The individual nutrients should be described one after the other and not switch between them several times.

AR: We modified the nutrient section for clarity

Line 285: Please insert some data.

Line 286: Do you mean the sum of pico- and nanophytoplankton?

Line 287-288: 92% of what? Recommendation: Picocyanobacteria determined by phycoerythrinfluorescence amounted 92% in GB and 96% in LB of the total picophytoplankton and was 30%

AR: We modified this paragraph according to the reviewer suggestion (L310-311)

Line 289: “The abundance of larger phytoplankton (>5 μm) was determined by microscopy”. The sentence can be deleted. It is described in the methods.

AR: This sentence was modified (L313)

Line 293: Filamentous unicellular cyanobacteria. A cyanobacteria filament always consists of more than one cell.

A: We thank the reviewer for this observation, “unicellular” was deleted

Line 292-293: "Cyanobacteria were 60% less abundant in the GB than in the LD." It is mentioned 2 sentences before. It can be deleted here.

AR: We deleted this sentence

Line 297: 95% of what

AR: We changed the sentence to "were more abundant in the GB than in LD (25% and 4% of the total phytoplankton respectively)"

Line 302: which layer is meant with the surface.

AR: With surface we referred to the upper 10 m of the water column. This was added to the text.

Line 316: . . .decreased quickly at 10m. . ." Rather: . . .decreased quickly below 10m. . .

AR: We thank the reviewer for this observation, the sentence was fixed

Line 318: The units of TEP and CSP should be explained in the methods.

AR: We add the units for TEP and CSP to the method section (L225-228)

Line 324: ". . .were only observed. . ." instead of ". . .were observed. . ."

AR: This has been modified.

Line 331: What is ESD? Please give the full name.

AR: We added equivalent spherical diameter to the text

Line 341: "POC flux slightly increased by 18% from the shallowest (40 m) to the deepest (180 m) depth. Fluxes of PN and CSP were higher at 40 and 60 m and decreased by 19 and 70% from 60 to 180 m. . .". I assume the layers 0-40m and 0-180m are meant.

AR: Yes, since we collected discrete samples at 40, 60, 110 and 180m, the assumption is that at each depth the sediment trap collected the particles formed and sinking from the euphotic zone.

Line 356: ". . .sediment traps at 110 m and 180 m. MnOx- like were They occurred as single particles and forming formed . . . and with other particles. . .".

AR: This has been modified.

Line 361: ". . .ranged from 0.6 to 16.5 mm (media mean 1.8) at 110 m (Table 4).

AR: We referred to the "median" as a measure of central tendency. The word "median" was fixed in the text

Line 371-381: These chapters would be easier to understand if data are inserted.

AR: We added the POC: PN ratio range to make the paragraph easier to follow.

Line 390: Please indicate in the method chapter how the DI has been calculated.

AR: We added the DI calculation to the method section (L240-244)

Line 300-401: “We assess the potential influence of increased O₂ concentration caused by the 2014/2015 MBI in the GB on the chemical composition and degradation stage of the sinking and suspended OM relative to the anoxic LD.” In my view, this is not clear enough in the ms, including the discussion.

Discussion The discussion involves a lot of repetition of the results.

Line 404-405 “...primary production”. Do you mean phytoplankton biomass? PP measurements were not included in this study.

AR: We replaced PP by phytoplankton biomass

Line 410-411: “Pico-phytoplankton cell abundance (cell mL⁻¹) dominated the small phytoplankton size fraction < 5µm (Table 2), suggesting a significant contribution to PP and Chl a concentration. This can not be deduced from the abundance alone.

AR: We deleted the sentence “suggesting a significant contribution to PP and Chl a concentration”

Line 421-422: “Cell abundance of total phytoplankton (>5 µm) were not significantly different (p=0.74) in the GB and the LD.” Which phytoplankton group refers to this statement. According to Table 3 the cell counts in both basins differed. I am wondering that the differences are not significant.

AR: To determine if the total phytoplankton abundances (considering all groups presented in table 3) were significantly different we used the Mann-Whitney U-test. The p-value (0.74) indicates that there is not sufficient evidence to indicate that the medians of those two data set were significantly different.

Line 434: “Our samples were collected right after the peak of the spring bloom. . . .”. That is not right. The spring bloom occurs, for example in the Gotland Basin, from the middle until the end of April (see also publications by B. Schneider et al.). The investigations were carried out in June.

AR: We corrected this paragraph.

Line 435-437: “. . .TEP concentrations had not reached the usually higher summer value yet since phosphate remained present in the water column (potentially not limiting the PP)”. Please make the relationship more clear.

AR: We modified this paragraph to make clear that even though we sample in June, the high Chl a concentration and the phosphate still present in the water column could indicate that PP was not nutrient limited yet. The presence of nutrients (phosphate) may be an explanation of why TEP concentration was lower than reported before for summer in the Baltic Sea when PP was low due to nutrient limitation.

Line 444: It should be noted at what depth the OMZ was located before the salt water inflow. Recommendation for rewriting the sentence: The MBI changed the vertical distribution of O₂ in the

GB by increasing its concentrations in depth below...m and relocation of the oxygen deficient layers from ..m to 74-140 m depth.

AR: We modified the text according to the reviewer recommendations

Line 452-453: "MBIs can have a major impact on nutrient recycling". Such general statements should be reduced throughout the ms.

AR: This sentence was moved to the beginning of the paragraph since was introducing the effect of MBI in nutrient distribution.

Line 480: ". . . Carbon flux below the euphotic zone. . .". To the bottom or to what depth?

AR: For clarification, this sentence was modified to "Our measurement of carbon flux at 40 m , below the euphotic zone, were..."

Line 485-486: ". . .the estimations based on our results from the GB are higher than the C fluxes predicted by those models." Here it should be taken into account that the measurements are obtained only from a single measurement over one or two days. The question is how representative a single measurement is. The subsequent paragraphs and chapter should be focused. At the moment it is very diffuse and the message is not clear.

AR: We agreed with the reviewer that our study represent only one discrete measurement; however, the objective of mention the results of previous estimations from modeling studies was precisely to add some context to our results.

We re-organize the discussion to make it clearer and more focus.

Table 3: It is not clear for me how the filamentous cyanobacteria were counted. Were the single cells in the filaments counted or were it counted as units of 50µm or 100µm length, as it is usually performed.

AR: The filamentous cyanobacteria were counted as single filament as it is usually performed. The word unicellular was deleted from the table.

Fig.2A: The scale of the x-Axis for salinity is wrong.

AR: We thank the reviewer for this observation; the salinity scale in figure 2a is fixed

In Fig. 4: It seems that only one or two depth are sampled. It should be indicated by zero-values if all depth are investigated and no particle is found.

AR: We added all values to figure 4, included the depths with zero particles.

Recommendation: Moderate revision Interactive comment on Biogeosciences Discuss., <https://doi.org/10.5194/bg-2018-360>, 201

Referee #2

Interactive comment on “Composition and Vertical Flux of Particulate Organic Matter to the Oxygen Minimum Zone of the Central Baltic Sea: Impact of a sporadic North Sea inflow”

by Carolina Cisternas-Novoa

T. Jilbert (Referee) tom.jilbert@helsinki.fi Received and published: 15 October 2018

In this study the authors use a wide range of analyses to investigate the vertical structure of suspended and sinking particulate matter composition in two stratified basins of the Baltic Sea following the MBI of 2014-2015. The data set is large and interesting, but I concur with the first reviewer’s assessment that the study lacks a clear focal message. For this reason I would encourage the authors to streamline the text when making their revisions.

My principal scientific comment about the paper would be that the authors have not acknowledged the possibility that vertical profiles of dissolved and particulate constituents in the Gotland Basin may be influenced by displacement effects. Following the MBI of 2014-2015, the sub-halocline water column of the GB experienced significant turbulent mixing between ‘old’ and ‘new’ water masses. A lot of the changes in water chemistry that occurred during 2015 were caused by displacement of old, stagnant water by water masses associated with the MBI (see e.g. Myllykangas et al., ESD 8, 2017). For example, the low concentrations of Si(OH)_4 and PO_4 in the deepest samples of the GB (Fig. 2A) are very likely due to enhanced contribution of oxic, low-nutrient water at this depth, and not due to scavenging of these constituents onto MnOx particles as suggested by the authors for phosphate (Line 464 and in the Conclusions). Displacement may have also influenced the vertical structure of suspended and sinking particulate matter, so this angle should be included when interpreting the results. In addition I would urge the authors to check their text thoroughly for typographic, spelling and grammatical errors. I have highlighted a few in my minor comments but there are likely several more.

AR: We agreed with the reviewer that the displacement effects associated with the 2104/2015 MBI might have influenced the vertical profiles of dissolved and particulate constituent. Therefore, we add this aspect to the discussion (L478-484) of the vertical profile of nutrients (L504-510), vertical profile of particulate organic in the water column, and particulate organic matter fluxes (L554-558).

However, even when we acknowledge that the net effect of the MBI in the particulate organic matter (POM) distribution and export efficiency is a combination of physical effects and biogeochemical changes; this does not modify our conclusion. Our results suggest that changes in the water chemistry related to the MBI and the consequent transport or in-situ formation of MnOx due to the favorable redox conditions may impact the distribution, degradation, and of export of POM in the GB

Kind regards, Tom Jilbert

Minor comments

Line 61: spelling: “allochthonous”

AR: We corrected the spelling mistake.

Line 95: spelling and grammar: the correct spelling is "Fårö"; Use "In the LD" rather than "At the LD"

AR: We corrected the grammar mistake

Line 110: rephrase (difficult to understand)

AR: We rephrased the sentence.

Line 156: grammar: Use "consisted of" rather than "consisted in"

AR: We changed the preposition

Line 166: what is the meaning of "caped"?

AR: We changed the word "capped" for "covered"

Line 181: grammar: Use "in duplicate" rather than "in duplicated"

AR: It has been fixed

Line 220: rephrase (difficult to understand)

AR: We rephrased the sentence

Line 321: spelling "below"

AR: We fixed the spelling of "below" in the ms

Line 354: what is the meaning of "and similar to the water column"?

AR: For clarity, we modified this sentence to "similar to the water samples,"

Line 356: word missing: "MnOx like were..."

AR: We fixed the sentence

Line 357: Remove colon (:) before "TEP"

AR: We removed the colon

Line 358: Define ESD

AR: We added the definition of equivalent spherical diameter (ESD) to the text.

Line 362: Avoid starting a sentence with an acronym

AR: This has been fixed

Line 375: add space before bracket. Also "Redfield's" should be "Redfield ratio"

AR: We fixed those mistakes

Line 390: DI should be introduced and defined in the Methods section

AR: We added the definition and calculation of the DI to the method section.

Line 432: grammar: “may be enhanced”

AR: We changed this line

Line 437: typographic errors

AR: We fixed the typographic error

Line 444: typographic errors

AR: We fixed the typographic error

Line 451: “compounds” plural

AR: We corrected the word to “compounds”

Line 453: spelling: “phosphorus”

AR: We corrected the spelling of “phosphorus” in the ms.

Line 464: Rephrase and check grammar, tenses, etc.

AR: We rephrase and corrected the grammar of this paragraph.

Line 468-470: these statements belong in Results rather than Discussion

AR: We moved the statement to the results section

Line 489-90: typographic errors

AR: We modified this paragraph and fixed the errors.

Line 519: Mn²⁺ is not an electron acceptor

AR: We fixed this mistake

Line 526: PN and CSP are not compounds. Rephrase.

AR: We changed “compounds” to “components of POM”

Line 597: Nisken bottle, not CTD

AR: We replaced CTD by Niskin bottle

Table 2: should the units be “cells/mL”?

AR: We modified how we showed the units to (cell ml⁻¹)

Fig. 4: are these all the sampling depths for MnOX-like particles? If samples from other depths were studied but yielded zero particles, these should also be included in the plot

AR: We added all values to figure 4, included the depths with low number or zero particles.

1 Composition and Vertical Flux of Particulate Organic Matter to the Oxygen Minimum Zone
2 of the Central Baltic Sea: Impact of a sporadic North Sea inflow

3

4

5 Carolina Cisternas-Novoa*, Frédéric A.C. Le Moigne, Anja Engel.

6 *GEOMAR, Helmholtz Centre for Ocean Research Kiel, Düsternbrooker Weg 20, D-24105*

7 *Kiel*

8 **Corresponding author:* Carolina Cisternas-Novoa, GEOMAR, Helmholtz Centre for Ocean

9 Research Kiel, Düsternbrooker Weg 20, D-24105 Kiel, Germany, +49 431 600-4146

10 ccisternas@geomar.de

11 Keywords: Baltic Sea, Oxygen minimum zone, POC, PN, POP, TEP, CSP, Sediment trap,

12 Export efficiency.

13

Abstract

Sinking particles are the main form to transport photosynthetically fixed carbon from the euphotic zone to the ocean interior via the biological carbon pump (BCP). Oxygen (O₂) depletion may improve the efficiency of the BCP. However, how the lack of O₂ mechanistically enhances particulate organic matter (POM) fluxes is not well understood. Here, we investigate distributions and fluxes of POM in two deep basins in the Baltic Sea (GB: Gotland basin and LD: Landsort Deep) with contrasting oxygenation regimes, resulting from a major oxygen-rich saltwater inflow event that oxygenated the bottom waters of GB but not the LD. In June 2015, we deployed surface tethered sediment traps in oxygenated surface waters (GB:40 and 60 m; LD: 40 and 55m), within the oxygen minimum zone (OMZ, GB: 110 m and LD: 110 and 180 m), and at deeper waters oxygenated by the inflow in GB (180 m). We hypothesize that the different O₂ conditions in the water column of the GB compared with the LD affected the POM distribution and caused differences in export efficiency between those two stations.

Fluxes and composition of sinking particles were different in the GB and the LD. In the GB, POC flux was 18% lower in the shallowest trap (40 m) than in the deepest sediment trap (at 180 m). Particulate nitrogen (PN) and Coomassie stainable particles (CSP) fluxes decreased with depth, and particulate organic phosphorus (POP), biogenic silicate (BSi), Chl *a*, and transparent exopolymeric particles (TEP) clearly peaked within the core of the oxygen minimum zone (OMZ, 110 m); this coincided with a high flux of manganese oxide (MnOx)-like particles. In the LD, POC, PN, and CSP fluxes decreased 28, 42 and 56% respectively from the surface to deep waters. POP, BSi and TEP fluxes, however, did not decrease with depth and were slightly higher in the 110 m sample. During this study, MnOx-like particle flux was two orders of magnitude higher in the GB (affected by the 2014/2015 North Sea inflow) relative to the LD.

Our results suggest that MnOx-like particles, formed after the inflow of oxygenated water into the GB, may form aggregates containing, not only transparent exopolymeric particles, as indicated previously, but also POC, POP, BSi, and Chl *a*. Aggregates composed of MnOx-like particles and POM may accumulate in the redoxcline, where they formed larger particles that eventually sink to

42 the seafloor. We propose that this mechanism would alter the vertical distribution and the flux of
43 POM, and it may contribute to the higher transfer efficiency of POC in the GB. This idea is
44 consistent with the fact that the OM reaching the seafloor was fresher and less degraded in the GB
45 than in the LD.

46 **1. Introduction**

47 Sinking particles are the primary vehicles for transporting photosynthetically fixed carbon from
48 the surface to the deep ocean via the BCP (Boyd and Trull, 2007; Turner, 2015). It has been
49 suggested that the transfer of particulate organic carbon (POC) from the euphotic zone to the
50 ocean interior is enhanced in oxygen minimum zones (OMZs) (Cavan et al., 2017; Devol and
51 Hartnett, 2001; Engel et al., 2017; Keil et al., 2016; van Mooy et al., 2002). Possible mechanisms
52 explaining the higher POC transfer include: i) the reduction of aggregate fragmentation due to the
53 lower zooplankton abundance within the OMZ (Cavan et al., 2017; Keil et al., 2016); ii) a higher
54 refractory nature of sinking particles (Keil et al., 2016; van Mooy et al., 2002); iii) a decrease in
55 heterotrophic microbial activity due to oxygen limitation (Devol and Hartnett, 2001); iv) the
56 preferential degradation of nitrogen-rich organic compounds (Kalvelage et al. 2013; Van Mooy et
57 al. 2002, Engel et al. 2017), and v) changes in ballast materials that may alter the sinking velocity
58 and protect organic matter from degradation (Armstrong et al., 2002). However, mechanisms of
59 how low O₂ concentration would affect the composition and fate of sinking OM, and the
60 efficiency of the biologic carbon pump in oxygen-deficient basins have hardly been investigated.

61 The semi-enclosed, brackish Baltic Sea is a unique environment with strong natural gradients of
62 salinity and temperature (Kullenberg and Jacobsen, 1981), primary productivity, nutrients
63 (Andersen et al., 2017), and O₂ concentrations (Carstensen et al., 2014a). New production,
64 defined as the fraction of the autotrophic production supported by allochthonous sources of
65 nitrogen (Dugdale and Goering, 1967) is considered equivalent to the particulate OM export
66 (Eppley and Peterson, 1979; Legendre and Gosselin, 1989) on appropriate timescales. In the
67 Baltic Sea, new production varies seasonally (Thomas and Schneider, 1999); spring and summer
68 are periods of elevated new production supported by the diatom-dominated spring bloom and by

69 diazotrophic cyanobacteria, respectively (Wasmund and Uhlig, 2003). Based on sediment trap
70 data, collected at 140 m depth in the Gotland Basin, Struck et al. (2004) reported that the highest
71 fluxes of POC occur in fall, followed by summer and spring. Using $\delta^{15}\text{N}$ they showed that during
72 the summer, N_2 fixation by diazotrophic species was the primary source (~41%) of the exported
73 nitrogen, and that the majority of the particulate OM sedimenting in the central Baltic Sea is of
74 pelagic origin.

75 OM export from the euphotic zone to the seafloor has a dual significance in the deep basins of the
76 Baltic Sea. On the one hand, it contributes to the long-term burial of POC, and consequently to
77 the removal and long-term storage of CO_2 from surface waters (Emeis et al., 2000; Leipe et al.,
78 2011); on the other hand, it connects the pelagic and the benthic systems contributing to the
79 oxygen consumption and hence deoxygenation at depth. Environmental and anthropogenic
80 changes may alter the magnitude and composition of OM transferred from the surface to the
81 seafloor in the Baltic Sea (Tamelander et al. 2017). The reduction of nutrient inputs as targeted by
82 the Baltic Marine Environment Protection Commission (HELCOM) can cause a decrease in OM
83 downward flux and limit the oxygen depletion. However, to fully suppress hypoxia enhanced
84 ventilation would be necessary the bottom waters of the Baltic Sea.

85 The Gotland Basin (GB), and the Landsort Deep (LD) are the deepest basins of the Baltic Sea.
86 They exhibit permanent bottom-water hypoxia (Conley et al. 2002), caused by a combination of
87 limited water exchange with the North Sea through the Kattegat Strait, strong vertical
88 stratification, and high production /rem mineralization of OM due to eutrophication (Carstensen et
89 al., 2014b; Conley et al., 2009). From the 1950s to 1970s, the hypoxic zones ($<60 \mu\text{mol O}_2 \text{ kg}^{-1}$) in
90 the Baltic Sea had expanded fourfold (Carstensen et al. 2014). Salt-water inflows from the North
91 Sea are the primary mechanism renewing deep water in the central Baltic Sea. A Major Baltic
92 Inflow (MBI) occurred in 2014/2015 (Mohrholz et al. 2015); this event ventilated bottom waters
93 for five months between February and July 2015 (Holtermann et al., 2017). The 2014/2015 MBI
94 caused the intrusion of O_2 to deep hypoxic waters, a substantial temperature variability
95 (Holtermann et al., 2017), the displacement of remnant stagnant water masses by new water that

106 | changed the chemistry of the water column (Myllykangas et al., 2017), and high turbidities that
107 | may be associated with redox reactions products (Schmale et al., 2016). At the time of sampling
108 | (June 2015), this MBI had reached the Gotland Basin , but did not affect the LD, located further
109 | northwest. In the LD, water properties did not change due to the MBI, the sulfidic layer was
110 | maintained (hydrogen sulfide, H₂S concentrations of 20.7- 21.2 μM), and salinity varied between
111 | 10.6 and 10.9 (Holtermann et al., 2017).

112 | In the GB and the LD, a permanent transition zone of about 2 to 10 m thickness separates the
113 | surface oxygenated and the oxygen-deficient waters; the approximated position of the pelagic
114 | redoxcline is between 127 and 129 m in the GB and between 79 and 85 m in the LD (Glockzin et
115 | al., 2014). The water column stratification is zone known as “pelagic redoxcline” is only
116 | disrupted by sporadic intrusions of saline, well-oxygenated waters from the North Sea (Günter et
117 | al., 2008). In the GB, the 2014/2015 MBI oxygenated the deep water column, removed the
118 | sulfidic waters in the deeper layers below the redoxcline, and created a secondary near-bottom
119 | redoxcline (Schmale et al., 2016). A steep redox gradient characterizes the pelagic redoxcline;
120 | here electron acceptors and their reduced counterparts are vertically segregated, and
121 | biogeochemical transformations mediated by microbial processes are actively occurring (Bonaglia
122 | et al., 2016; Brettar and Rheinheimer, 1991; Neretin et al., 2003). For instance, iron (Fe) and
123 | manganese (Mn) undergo rapidly reversible transformations at the redox interface. Under anoxic
124 | conditions, these metals are present in dissolved reduced forms Mn(II) and Fe(II); under oxic
125 | conditions or in presence of nitrate they react with O₂ and form particulate oxides. Manganese
126 | oxides (MnOx) production may be microbially mediated (Neretin et al., 2003; Richardson et al.,
127 | 1988), or authigenic (Glockzin et al., 2014). The reduction of Mn(IV) with sulfide occurs within a
128 | scale of seconds to minutes (Neretin et al., 2003), and is inhibited by nitrate (Dollhopf et al.,
129 | 2000). The sporadic oxygenation of the deep water of the GB combined with the release of Mn
130 | from the sediments into the water column (Lenz et al., 2015) generate appropriate conditions for
131 | particulate MnOx formation. MnOx particles have previously been observed in pelagic
132 | redoxclines in the Baltic Sea (Glockzin et al., 2014; Neretin et al., 2003). They are amorphous or

123 star-shaped particles that can occur as single particles or form aggregates enriched in OM (Neretin
124 et al., 2003), specifically with transparent exopolymer particles (TEP) (Glockzin et al., 2014).
125 TEP are highly sticky, polysaccharide-rich particles that can enhance aggregation and the
126 formation of marine snow (Engel, 2000; Logan et al., 1995). Thus, MnOx-OM aggregates may
127 significantly contribute to the downward flux of POC. However, TEP are less dense than seawater
128 (Azetsu-Scott and Passow, 2004); therefore they could also reduce the density of marine
129 aggregates and decrease their sinking velocity if the ratio of dense particles to TEP is too small
130 (Azetsu-Scott and Passow, 2004; Engel and Schartau, 1999; Mari et al., 2017). Mixed aggregates
131 containing MnOx and TEP have reported before for the GB and LD (Dellwig et al. 2010;
132 Glockzin et al. 2014). Their sizes ranged between 0.8 and 41 μm equivalent spherical diameter
133 (ESD), and their sinking velocity (0.76 m d^{-1}) was lower than what was predicted by the Stokes'
134 law (Glockzin et al., 2014) possibly due to their star-shaped morphology and the high OM content
135 attached to them. Additionally, MnOx aggregates may affect the cycling of particle-reactive
136 elements like phosphorus and trace metals via scavenging processes (Dellwig et al., 2010). To
137 date, there are no measurements of the density of MnOx-OM aggregates, their potential ballast
138 effect of sinking OM, or their effect on the flux of particle-reactive elements in the Baltic Sea.

139 The objectives of this study are, first, to characterize the amount and composition of particles
140 sinking out of the euphotic zone in two deep basins of the Baltic Sea: the GB and the LD. Second,
141 to study how the oxygenation of deep waters (below 140 m) in the GB caused by the 2014/2015
142 MBI will affect the sinking fluxes of POM compared with LD that was not affected by the MBI
143 and exhibited low O₂ concentration (below 74 m) and sulfidic conditions (below 160 m) in the
144 deep water. We hypothesize that the MBI that altered the water column chemistry and created
145 different O₂ conditions in the GB compared with the LD affected the abundance and in-situ
146 formation of MnOx rich-aggregates and subsequently OM distribution causing differences in
147 degradation and export of OM between those two stations.

148 **2. Methods**

149 *2.1. Sampling location and water column properties*

150 Samples were collected during the BalticOM cruise in the Baltic Sea onboard the *RV Alkor* from
151 June 3th to June 19th, 2015. We collected sinking particles using surface-tethered sediment traps
152 (Engel et al., 2017; Knauer et al., 1979) in the GB and the LD (Fig.1). Additionally, water column
153 samples (table 2) were collected using a Niskin-bottle rosette at the locations of the trap
154 deployments. Temperature, salinity and O₂ concentration were determined at each station using a
155 Sea-Bird (CTD) probe equipped with a oxygen (Oxyguard, PreSens), calibrated with discrete
156 samples measured using the Winkler method (Strickland and Parsons, 1968; Wilhelm, 1888).

157 2.2. Sediment trap design and deployment

158 We deployed two surface-tethered sediment traps for two days in the GB, and one day in the LD
159 (Fig.1). Each trap collected particles at four depths 40, 60 (55 in LD), 110 and 180 m (Table 1) to
160 estimate POM fluxes to and within the OMZ. The sediment trap consisted of five (two traps were
161 located at 40 m in each station to evaluate replicability) arrays of 12 acrylic particle interceptor
162 tubes (PITs) mounted in a PVC cross frame; each tube was equipped with an acrylic baffle at the
163 top to minimize the collection of swimmers (Engel et al., 2017; Knauer et al., 1979). The PITs
164 were 7 cm in diameter and 53 cm in height with an aspect ratio of 7.5 and a collection area of
165 0.0038 m². The cross frame and PITs were attached to a line that had a bottom weight and a set of
166 surface and subsurface floats. The procedures for PIT preparation and sample recovery followed
167 Engel et al. (2017). Shortly before deployment, each PIT was filled with 1.5 L of seawater
168 previously filtered through a 0.2 µm pore size cartridge. A preservative solution of saline brine
169 (50 g L⁻¹) was added slowly to each PIT underneath the 1.5 L of filtered seawater, carefully
170 keeping the density gradient. The PITs were kept covered until deployment and immediately after
171 recovery to avoid contamination. After recovery, the density gradient was visually verified, and
172 the supernatant seawater was siphoned off the PIT. Then, the remaining bottom waters (approx.
173 0.6 L) containing the particles were pooled together and filled-up to 10 L with filtered seawater.
174 After that, the samples were screened with a 500 µm mesh to remove swimmers. Subsequently,
175 samples were split into aliquots that were processed for the different biogeochemical analysis as
176 described in Engel et al. (2017).

2.3. Biogeochemical analysis

Nutrients were measured in seawater samples of the deployment stations. Ammonium (detection limit 0.05 μM) was measured directly on unfiltered seawater samples on board after Solórzano (1969). Phosphate, nitrate, and nitrite (detection limit 0.04 μM) were filtered through a 0.2 μm pore size and stored frozen until their analysis; samples were measured photometrically with continuous flow analysis on an auto-analyzer (QuAatro; Seal Analytical) after Grasshoff et al. (1999).

Particulate organic carbon (POC), nitrogen (PN), organic phosphorus (POP), and chlorophyll *a* (Chl *a*) were determined as described in Engel et al. (2017). Aliquots of 100 to 200 ml of the trapped material, and 500 ml for the sampled seawater were filtered in duplicate for each parameter at low vacuum (<200 mbar), onto pre-combusted GF/F filters (8h at 500°C). After filtration, the filters were stored frozen (-20°C) until analysis. Prior analysis, filters for POC-PN determination were exposed to acid fumes (37% hydrochloric acid) to remove carbonates, and subsequently dried for 12h at 60 °C. POC and PN concentrations were determined using an elemental analyzer (Euro EA, Hechatech) after Sharp (1974).

POP was analyzed after Hansen and Koroleff (1999). POP was oxidized to orthophosphate by heating the filters in 40 mL of deionized water (18.2M Ω) with Oxisolv (MERCK 112936) for 30 min in a pressure cooker. Orthophosphate was determined spectrophotometrically at 882 nm in a Shimadzu UV-VIS Spectrophotometer UV1201.

Chl *a* was analyzed after extraction with 10 mL of 90% acetone, the fluorescence of the samples was measured using a Turner fluorimeter (440/685 nm, Turner, 10-AU) according to Strickland et al. (1972). The fluorometer was calibrated with a standard solution of Chl *a* (Sigma-Aldrich C-5753).

Phytoplankton composition and abundance in the stations where we deployed sediment traps were evaluated using light microscopy and flow cytometry. Phytoplankton, > 5 μm , was counted and identified in 50 ml of fixed samples (Lugol's solution, 1% final concentration) using a Zeiss Axiovert inverted microscope (200x magnification). The size of the counted phytoplankton

204 species ranged from 10 to 200 μm . Phytoplankton, $<20 \mu\text{m}$, cell abundance was quantified using a
205 flow cytometer (FACSCalibur, Becton, Dickson, Oxford, UK). 2 ml samples were fixed with
206 formaldehyde (1% final concentration) and stored frozen ($-80 \text{ }^\circ\text{C}$) until analysis (two weeks later).
207 Cell counts were determined with CellQuest software (Becton Dickenson); pico- and
208 nanoplankton populations of naturally containing chlorophyll or phycoerythrin (*i.e.*,
209 *Synechococcus*) were identified and enumerated.

210 Biogenic silica (BSi) was determined by filtering duplicate aliquots of 50 to 100 mL onto $0.4 \mu\text{m}$
211 cellulose acetate filters. Samples were stored at -20°C until analysis. For the measurements, filters
212 were digested in NaOH at 85°C for 135 min; the pH was adjusted to 8 with HCl. Silicate was
213 measured spectrophotometrically according to Hansen and Koroleff (2007).

214 Transparent exopolymeric particles (TEP) and coomassie stainable particles (CSP) from trap and
215 water column were analyzed by microscopy according to Alldredge et al. (1993) and Long and
216 Azam (1996) respectively. Duplicate aliquots of 5 to 20 ml were filtered onto $0.4 \mu\text{m}$ Nuclepore
217 membrane filters (Whatmann) and stained with 1 ml of Alcian Blue solution for TEP and
218 Coomassie brilliant blue solution for CSP. Filters were transferred onto Cytoclear $\text{\textcircled{R}}$ slides and
219 frozen (-20°C) until microscopy analysis. For the analysis, thirty images for each filter were
220 captured under 200x magnification using a light microscope (Zeiss Axio Scope A.1) connected to
221 a color camera (AxioCam MRc). Particle abundance and area were measured semi-automatically
222 using an image analysis system including the WCIF ImageJ software. The RGB was split in three
223 channels: red, blue and green, and the red was used to quantify the amount of TEP and CSP
224 (Engel 2009). Additionally, TEP and CSP in water samples from the stations where we deployed
225 sediment traps were analyzed spectrophotometrically (with higher vertical resolution than
226 microscopy) according to Passow and Alldredge (1995) and Cisternas-Novoa et al. (2014)
227 respectively. Concentrations of TEP are reported relative to a xanthan gum standard and
228 expressed in micrograms of xanthan gum equivalents per liter ($\mu\text{g XG eq. L}^{-1}$), and concentrations
229 of CSP are reported relative to a bovine serum albumin standard and expressed in micrograms of
230 bovine serum albumin equivalents per liter ($\mu\text{g BSA eq L}^{-1}$).

231 [The abundance of MnOx-like particle](#) was determined [by image analysis](#), using the same images
232 that for TEP and CSP [analysis](#) and a [modified version](#) of the method described above. Thirty
233 images per filter (200x) were analyzed semi-automatically using Image J. [The blue](#) channel was
234 used to quantify the amount of MnOx-like particles in the water column and sediment traps, in
235 this [manner](#), the MnOx-like particles were clearly visible with a negligible disruption from TEP
236 or CSP stained blue.

237 Total amino acids (TAA) were analyzed in unfiltered seawater and trapped material. Samples
238 were stored at -20°C until analysis. Duplicate samples were hydrolyzed at 100 °C in 6N HCl
239 (Suprapur® Hydrochloric acid 30%) and 11 mM ascorbic acid for 20h. Amino acids were
240 separated and measured by high-performance liquid chromatography (HPLC), after derivatization
241 with ortho-phthaldialdehyde using a fluorescence detector ([Excitation/Emission 330/445 nm](#))
242 (Dittmar et al., 2009; Lindroth and Mopper, 1979). [The quantitative degradation index \(DI\) of](#)
243 [Dauwe et al. \(1999\), based on changes in amino acids composition of the POM as it undergoes to](#)
244 [degradation processes in the water column, was calculated using the factor coefficient of Dauwe](#)
245 [et al. \(1999\) and the average and standard deviation of the TAA of this data set.](#)

246
247 Total combined carbohydrates (TCHO) were determined by ion chromatography according to
248 Engel and Händel (2011). TCHO were analyzed in the unfiltered seawater and sediment trap
249 material. Samples were stored at -20°C until analysis. Prior to analysis, the samples were desalted
250 by membrane dialysis using dialysis tubes with 1 kDa molecular weight cut-off (Spectra Por). The
251 desalination was conducted for 4.5 h at 1°C. Then, a 2 mL subsample was sealed with 1.6 mL 1M
252 HCl in pre-combusted glass ampoules and hydrolyzed. Samples were hydrolyzed for 20 h at
253 100°C. After hydrolysis, the subsamples were neutralized by acid evaporation under N₂
254 atmosphere at 50°C, resuspended with ultrapure Milli-Q water and analyzed by ion
255 chromatography.

256 *2.4 Statistics*

257 Significant differences between two parameters were tested using the Mann-Whitney U-test. The
258 results of statistical analyses were assumed to be significant at p -values < 0.05 . Statistical
259 analyses were performed using Matlab software (MatlabR2014a).

260 3. Results

261 3.1. Biogeochemistry of the water column

262 The water column of both stations was stratified during the study. In the GB the seasonal
263 thermocline was located between 22 and 37 m, the temperature decreased rapidly from 9.8°C in
264 the surface mix layer to 4.7°C below 37 m. Deeper in the water column, a pycnocline (halocline)
265 coincided with the oxycline and was located between 65 m (S=7.6) and 80 m (S=10.2), below 80
266 m the salinity gradually increased up to 13.5 at the bottom (220 m). In the GB, a hypoxic layer
267 (<40 $\mu\text{mol O}_2 \text{ L}^{-1}$) was located between 74 and 140 m; the core of the OMZ (<10 $\mu\text{mol O}_2 \text{ L}^{-1}$)
268 was located between 96 and 125 m. The O_2 concentration increases from 35 $\mu\text{mol O}_2 \text{ L}^{-1}$ at 140 m
269 to 79 $\mu\text{mol O}_2 \text{ L}^{-1}$ at 220 m (Fig. 2a). In the LD, the seasonal thermocline was located between 10
270 and 39 m, where the temperature decreased gradually from 12°C to 4.0°C (Fig. 2b). The
271 pycnocline was between 55 (S=7.2) and 75 m (S=9) below that the salinity is constant (S=10.7)
272 until the bottom of the station (430 m). The O_2 concentration was below the detection limit (<3
273 $\mu\text{mol O}_2 \text{ L}^{-1}$) from 74 m to the bottom.

274
275 The vertical profile of nutrients was different at both stations (Fig. 2). In the GB, nitrate
276 concentration increased from below the detection limit, in the upper ten meters, to
277 0.17 μM at 40 m (Fig. 2a). Concentrations were variable within the OMZ with 6 μM in
278 the upper (80 m) and lower oxycline (140 m), and 0.12 μM in the core of OMZ (110 m);
279 the nitrate concentration decreased to 4.8 μM in the deepest sample (220 m). Nitrite was
280 below the detection limit in most of the water column except for 60 m (0.09 μM) and 110
281 m (0.11 μM). Ammonium increased from 0.14 μM in upper ten meters to 1.15 μM at 40
282 m; concentrations were variable in the OMZ with less than 0.15 μM in the upper (80 m)

283 and lower oxycline (140 m), and maximum concentration of $3.28 \pm 0.01 \mu\text{M}$ in the core
284 of the OMZ (110m). Vertical profiles of phosphate and silicate at the GB were similar;
285 the concentrations steadily increased from the upper ten meters of the water column
286 (0.29 μM and 10.36 μM respectively) to the OMZ (2.67 μM and 39.07 μM respectively),
287 and gradually decreased below the OMZ (Fig. 2a). Hydrogen sulfide was not detectable
288 in the GB.

289 In the LD, nitrate and nitrite concentrations were below the detection limit between the surface
290 and 250 m ($<0.04 \mu\text{M}$) (Fig. 2b). Nitrite showed a maximum of 0.22 μM at 350 m, and nitrate a
291 maximum of 6.0 μM at 400 m. Ammonium concentrations varied between 0.06 and 0.59 μM in
292 the upper 70 m and increased to 5.97 and 8.03 μM in the OMZ (below 74 m). The lowest
293 concentration (0.07 μM) was measured in the surface and maximum concentration of 8.03 μM at
294 110 m. Phosphate and silicate concentrations were relatively low within the mixed layer due to
295 phytoplankton consumption; gradually increased below the pycnocline, and decreased between
296 110 and 180 m. Phosphate concentrations varied between 1.5 and 2.5 μM in the upper 110 m of
297 the water column, decreased to 0.22 μM at 180 m and increased to 2.7 μM at 430 m (deepest
298 sample). Silicate ranged between 25 and 38 μM in the upper 110 m of the water column,
299 decreased to 7.4 μM at 180 m, and increased 38.9 μM at 430 m of the water column. Hydrogen
300 sulfide was detectable below 180 m, with the highest concentration (3.97 μM) at 250 m and the
301 lowest (0.04 μM) between 300 and 350 m (Fig. 2b).

302 *3.2. Particulate organic matter concentration in the water column*

303 Chl *a* concentration in the upper 10 m was slightly higher in the GB (1.5-1.7 $\mu\text{g L}^{-1}$, Fig. 3b) than
304 in LD (1.4-1.2 $\mu\text{g L}^{-1}$ and 0.1-0.3 μM , Fig. 3e). In both stations, more than 90% of the total
305 smaller phytoplankton (<20 μm , pico- and nanophytoplankton) abundances, determined by flow
306 cytometry, were measured in the upper 60 m, although phytoplankton was detectable in the entire
307 water column. Pico- and nanophytoplankton abundances were 10% higher in GB than in LD
308 (Table 2). Picocyanobacteria determined by phycoerythrin fluorescence account for 92% and 96%

309 | of the total picophytoplankton in GB and LD respectively. Picrocyanobacteria was 30% higher in
310 | GB than in LD.

311 | Large phytoplankton (>5 µm) abundance, determined by microscopy, was 63% higher in the LD
312 | than in the GB (Table 3). Filamentous cyanobacteria dominated the large phytoplankton
313 | community at both stations with up to 90% corresponding to *Aphanizomenon* sp. Cyanobacteria
314 | represented 56% of the total phytoplankton counts in the GB and up to 74% in the LD.

315 | Dinoflagellates (dominated by *Dinophysis* sp.) were significant in both stations (19% of the total),
316 | whereas chlorophytes (dominated by filaments of *Planctonema* sp. containing cylindrical cells)
317 | were more abundant in the GB than in LD (25% and 4% of the total phytoplankton respectively).
318 | Diatoms represented less than 1% of the phytoplankton in both stations, and they were slightly
319 | more abundant at 40 m in the LD (Table 3). BSi was higher in the upper 10 m (0.4-0.5 µM) and
320 | decreased with depth in the GB (Fig. 3b), whereas in the LD, BSi showed a peak at 40 m and then
321 | decreased with depth (Fig. 3f).

322 | Vertical profiles of POC, PN, and POP concentration were similar in the water column of the two
323 | stations (Fig. 3a, d). In the GB, the concentrations were higher in the upper 10 m of the water
324 | column (POC: 40.38 ± 0.80 , PN: 3.89 ± 0.01 , and POP: 0.26 ± 0.04 µM) and decreased gradually
325 | with depth until 110 m where relatively high concentrations (POC 18 ± 0.63 , PN: 2 ± 0.08 , and
326 | POP: 0.2 µM) were observed. The lowest concentrations were found at 180 m (POC: $11.97 \pm$
327 | 1.03 , PN: 1.05 ± 0.02 , and POP <0.03 µM) (Fig. 3a). In the LD, POM decreased with depth from
328 | the surface (POC: 35 ± 0.99 , PN: 4 ± 0.09 , and POP: 0.2 µM) to 40 m, remained relatively
329 | constant between 40 and 80 m and decreased again between 110 and 250 m (Fig. 3d).

330 | We observed high concentrations of TEP and CSP in the upper 10 m in both stations. The highest
331 | TEP concentration was measured at 1 and 10 m at both stations, and it was slightly higher (19%)
332 | in the GB than in the LD (Fig. 3c, f). TEP and CSP vertical profiles were different from each
333 | other in the GB (Fig. 3c) and covaried in the LD (Fig. 3f). Like observed for POC, PN, and POP,
334 | TEP concentrations showed a peak at 110 m (50.29 ± 6.17 µg XG eq. L⁻¹) in the GB. The highest
335 | concentration of CSP at this station was observed in the shallowest (1 m) sample, CSP

336 concentration decreased quickly below 10 m, and then it increased at 140 and 230 m (the deepest
337 sample ~20 m above the seafloor) (Fig. 3c). In the LD, the highest concentrations of TEP and
338 CSP were measured in surface (1 and 10 m) and at 110 m (Fig. 3f). TEP and CSP decreased with
339 depth in the first 80 m (from 53.26 ± 7.10 to 18.39 ± 4.57 $\mu\text{g XG eq. L}^{-1}$ and from 53.26 ± 7.10 to
340 31.57 ± 18.78 $\mu\text{g BSA eq. L}^{-1}$). Both types of gel-like particles showed an increase in
341 concentration at 110 m (49.25 ± 4.08 $\mu\text{g XG eq. L}^{-1}$ and 66.89 ± 22.33 $\mu\text{g BSA eq. L}^{-1}$
342 respectively). Below 110 m, TEP concentrations stayed relatively constant, while CSP
343 concentrations decreased at 180 m and kept relatively constant below that depth.

344 *3.3. MnOx-like particles vertical distribution in the water column*

345 Dark, star-shaped, MnOx-like particles (Glockzin et al., 2014; Neretin et al., 2003) were only
346 observed below the fully oxygenated mixed layer in the GB and, in less abundance, in the LD
347 (Fig. 4). In GB, single MnOx-like particle and large aggregates were observed from 80 m to 220
348 m (the deepest sample, approximately 28 m above the seafloor). Relatively high concentration of
349 MnOx-like particles (2×10^6 particles L^{-1}), were measured in the upper (80 m) and lower (140 m)
350 oxycline where the O_2 concentration was less than $40 \mu\text{M}$, and at 220 m (4×10^6 particles L^{-1}) (Fig.
351 4a). The lowest abundance of MnOx-like particles (7×10^5 particles L^{-1}) was observed at 110 m, in
352 the core of the OMZ where the O_2 concentration was less than $10 \mu\text{M}$. The equivalent spherical
353 diameter (ESD) varied between 0.6 and $30.5 \mu\text{m}$ and the median was $3.0 \mu\text{m}$. The largest
354 aggregates were observed in the upper oxycline (80 m). In the LD, MnOx-like particles were less
355 abundant, smaller and had a narrow distribution in the water column than in the GB. MnOx-like
356 particles were not detected in the fully oxic (0-40 m) or fully anoxic (180 to 430 m) water
357 column. At 60 m, right above the oxycline, MnOx-like particles began to appear, however, in
358 relatively low abundance. The maximum abundance, 9×10^5 particles L^{-1} , was observed in the
359 oxycline at 70 m (Fig. 4b). The ESD varied ranged between 0.6 and $13.4 \mu\text{m}$, the largest
360 aggregates were observed at 70 m.

361 *3.4. Fluxes of Particulate Organic Matter*

362 Fluxes of POC and PN varied little with depth in the GB (Fig. 5a-b). POC flux slightly increased (18%) from the shallowest (40 m) to the deepest (180 m) sediment trap. Fluxes of PN and CSP
363 were higher at 40 and 60 m and decreased (19 and 70 %) from 60 to 180 m, respectively (Fig. 5a
364 and 5c). On the other hand, fluxes of POP, BSi, Chl *a* (Fig. 5b) and TEP (Fig. 6a) peaked in the
365 sediment trap located in the core of the OMZ (-110 m). The increment of fluxes at 110 m
366 coincided with the presence of abundant MnOx-like particles associated with TEP (Fig. 6a). In
367 addition, TEP size distribution, determined by image analysis, indicated an increase in large TEP
368 at 110 m (data not shown). In contrast, in the LD, POC, PN (Fig. 5d) and CSP (Fig. 6d) fluxes,
369 steadily decreased with depth by 28, 42 and 56% from 40 to 180 m. Similar to the fluxes
370 measured in the GB, the POP, BSi (Fig. 5e) and TEP (Fig. 6c) showed a smaller peak in the
371 sediment trap located at 110 m.
372
373 MnOx-like particles were drastically less abundant in sediment trap samples from the LD than in
374 the GB and when present, they appear as single particles, not aggregated with TEP or CSP (Fig.
375 6c, d). At both stations, and similar to the water column samples, MnOx-like particles were not
376 observed in sediment trap samples collected, in fully oxygenated depths (40 and 60 m). The flux
377 of MnOx-like particles at 110 and 180 m was two orders of magnitude larger in the GB than in
378 the LD (Table 4). In the GB, MnOx-like particles were present in the sediment traps at 110 m and
379 180 m. They occurred as single particles and forming aggregates with each other and other
380 particles such as TEP (Figure 6a,e), phytoplankton cells, or detrital material. The ESD of MnOx-
381 like particles and aggregates ranged from 0.6 to 167 μm (median 2.8 μm) at 110 m and from 0.6
382 to 153 μm (median 3.3 μm) at 180 m. In the LD, only a few, single MnOx-like particles were
383 observed at 110, their size ranged from 0.6 to 16.5 μm (median 1.8) (Table 4).
384 Total hydrolyzable amino acids (TAA) flux ranged from 371 ± 12 to $501 \pm 33 \mu\text{mol m}^{-2}\text{d}^{-1}$ in the
385 GB and from 502 ± 84 to $785 \pm 54 \mu\text{mol m}^{-2}\text{d}^{-1}$ in the LD (Fig. 7a). In the GB, the flux decreased
386 with depth whereas, in the LD, the TAA flux at 40 m was lower than at 60 m and decreased with
387 depth from 60 to 180 m (Fig. 7b). Vertical profile of TCHO flux was similar in both stations. The
388 TCHO flux varied between 303 ± 8 and $428 \pm 14 \mu\text{mol m}^{-2}\text{d}^{-1}$ in the GB (Fig. 7a) and between

389 503± 19 and 584± 8 $\mu\text{mol m}^{-2}\text{d}^{-1}$ in the LD (Fig. 7b). In both stations, TCHO flux increased from
390 40 to 110 m, where the highest TCHO flux was measured, and then TCHO flux decreased at 180
391 m. The TCHO flux at 180 m was 22% higher than at 40 m in the GB, and the same that at 40 m in
392 the LD.

393 3.5. Chemical composition of sinking and suspended OM

394 The molar ratios of suspended and sinking OM may be compared to the classical Redfield ratio
395 for living plankton (106C: 16N: P; Redfield et al., 1963). Sinking OM was slightly above
396 Redfield ratios at both stations. The POC:PN ratio of the sinking OM in both GB and LD were
397 not significantly different. In the GB, the POC:PN ratio of the sinking OM increased with depth
398 from 9.8 to 12.6. Contrastingly, in the suspended OM, POC:PN ratios were higher in the GB
399 compared to the LD ($p<0.001$; Mann–Whitney U-test). In the GB, the POC:PN ratio of suspended
400 OM varied between 8.4 and 12 without a clear trend with depth; while in the LD, decreased with
401 depth from 8.7 (at 1m) to 6.2 (at 400m), and a slightly higher value of 7.8 was observed at 430 m.

402 In the LD the POC:PN of sinking OM was significantly lower than in suspended OM ($p<0.001$).

403 The POC:POP molar ratio of sinking OM was lower ($p<0.05$) in the GB than in the LD; and it
404 was higher ($p<0.01$) in sinking than in suspended OM in the LD (Table 5). The POC:BSi molar
405 ratio was lower in sinking than in suspended OM in both stations (GB: $p<0.05$; LD: $p<0.01$). In

406 sinking OM, the POC:BSi ratio was below Redfield value, whereas in suspended OM it was

407 above Redfield ratio (Table 5). The PN:POP molar ratio was lower in sinking OM than in
408 suspended OM in both stations ($p<0.001$). In sinking OM this value was always below the
409 Redfield ratio, while in suspended OM, it was always above the Redfield ratio.

410 At both stations, the fraction of sinking POC composed of AA was larger than in suspended OM.

411 Similarly, the C contained in CHO made up a larger percentage in sinking OM than in suspended
412 OM (Table 5). The amino acid-based degradation index (DI, Dauwe et al., 1999) in sinking OM
413 varied from 0.1 to 1.14 and was higher than in suspended OM (-1.25 to -0.42). The DI was higher
414 in the GB than in the LD in sinking and suspended OM. In the sinking OM of the GB, the DI
415 decreased with depth but in the LD was more positive at 110m than at 60 m (Table 5).

416 4. Discussion

417 In this study, we described the results of 1) the characterization of the surface biogeochemical
418 conditions and the sinking particles produced in the euphotic zone of the GB and the LD, during
419 early summer 2015, 2) the flux, and vertical profile of sinking and suspended particles in the two
420 basins. Our results suggested that the intrusion of oxygenated water to the GB associated with the
421 2014/2015 MBI caused changes in the water chemistry that affected the chemical composition
422 and degradation stage of the sinking and suspended OM. This resulted in differences in the
423 composition and magnitude of the sinking particle flux between GB and LD.

424 *4.1 Characterization of biogeochemical conditions in GB and LD*

425 Temperature, O₂, and inorganic nutrient concentrations were similar in euphotic zone (upper 20
426 m) at both stations. Moreover, though there were slight differences in biogeochemical conditions,
427 such as phytoplankton biomass, phytoplankton composition and concentration and chemical
428 composition of POM, in the surface water column, those were not significant. The concentration
429 of Chl *a* (Fig. 3) and the abundance of picophytoplankton and nanophytoplankton (Table 2) were
430 slightly higher (20 and 10 % respectively) in the GB than in the LD. This agrees with estimates of
431 integrated total primary production, which were 10% larger in the GB (380 mg C m⁻² d⁻¹) than in
432 the LD (334 mg C m⁻² d⁻¹; Piontek et al., unpublished). At both stations, picophytoplankton
433 dominated the small phytoplankton (Table 2). These findings coincide with what was described
434 previously for early summer, in the Baltic Sea that indicate that during this period the productivity
435 is sustained mostly by nano- and picophytoplankton communities (Leppänen et al., 1995) which
436 co-existed with cyanobacteria and other phytoplankton species (Kreus et al. 2015). Microscopic
437 analysis of larger phytoplankton (>5 µm), on the other hand, showed that filamentous
438 cyanobacteria *Aphanizomenon* sp. (up to 200 µm large) was the dominant type on this size
439 fraction in the upper 40 m (Table 3). *Aphanizomenon* sp. and *Nodularia spumigena*, are known to
440 form summer blooms in the Baltic Sea, where they accumulate at the sea surface of the thermally
441 stratified water column (Bianchi et al., 2000; Nausch et al., 2009; Wasmund, 1997). The medians
442 of the cell abundance of total phytoplankton (>5 µm, table 3) in the upper 40 m of the water
443 column were not significantly different ($p=0.74$) in the GB and the LD.

444 POC, PN, POP, BSi were slightly higher in the surface waters of the GB than in the LD; while ,
445 TEP and CSP concentrations in the surface waters were similar at both stations (Fig. 3). The
446 concentration of TEP was higher than of CSP, both types of gel-like particles were most abundant
447 in the euphotic zone indicating a phytoplankton origin. In the surface water column, TEP
448 concentrations (48 and 62 $\mu\text{g X.G. Eq. L}^{-1}$ in the GB and the LD, respectively) were 69 and 76%
449 lower than the value previously reported for summer in the central Baltic Sea in June (200 μg
450 X.G. Eq. L^{-1}) (Engel et al., 2002). Likewise, our dissolved inorganic nitrogen concentrations were
451 below the detection limit in the surface; however phosphate concentrations were higher (0.2-0.65
452 μM) than the ones on the Engel et al. (2002) study. Mari and Burd (1998) reported that TEP
453 concentration peaked during the spring bloom and in summer in the Kattegat. TEP production
454 may be enhanced by environmental conditions such as nutrient limitation (Mari et al., 2005;
455 Passow, 2002), which are characteristic of late summer in the Baltic Sea (Mari and Burd 1998).

456 Surface satellite-derived Chl-a concentrations in the Gotland Deep indicate that our samples were
457 collected during Chl-a peak in mid-June (8–10 $\mu\text{g L}^{-3}$). Chl-a concentrations increased constantly
458 from mid-May to the sampling period (Le Moigne et al., 2017), thus, likely TEP concentrations
459 had not reached the usually higher summer value yet since the high concentration of Chl-a and
460 presence of phosphate in the water column may suggest that the PP was not nutrient limited).

461 Another possible explanation for the rather low concentrations of TEP could be that TEP may be
462 removed from the surface by aggregation and subsequent sedimentation during the spring bloom
463 due to the high abundance of cells and detrital particles during this time (Engel et al., 2002).

464 Although the composition and amount of OM in the surface waters at the two trap stations were
465 similar, below the euphotic zone (40 m) the vertical profile of nutrients and POM concentrations
466 were clearly different; likely due to the 2014/2015 MBI (Holtermann et al., 2017) that reached the
467 deep waters of the GB. This inflow changed the salinity in the deepest waters and the vertical
468 distribution of O_2 increasing its concentrations below 140 m and constraining the oxygen-deficient
469 layers from 74 m to 140 m depth. The water intrusion showed similar features as the new water
470 masses and water pushed out of the Bornholm Basin (Schmale et al., 2016). The combination of

471 physical effects (the displacement of water masses, turbulent mixing and lateral transport) and the
472 consequent development of redox conditions through 2015 may have impacted the distribution of
473 MnOx and POM in the GB. In contrast, the LD maintained permanent suboxic ($<5 \mu\text{mol L}^{-1}$)
474 waters below 74 m and hydrogen sulfide was detectable at 180 and 250 m (Fig. 2).

475 MBIs can have a major impact on nutrient recycling. In the GB nitrate concentration increased
476 possibly as a consequence of the oxidation of reduced nitrogen compounds (e.g., ammonium,
477 ammonia and organic nitrogen compounds like urea) (Le Moigne et al., 2017) that accumulated
478 during the stagnation (anoxic) period previous to the MBI (Hannig et al., 2007). Phosphorus
479 could bind to iron hydroxides and MnOx and settle down during oxic conditions, building up a
480 phosphate pool in the sediments that later on when the O_2 decreases close to the sediments, it may
481 become a source of phosphate (Gustafsson and Stigebrandt, 2007). In addition to changes in O_2
482 concentration, the MBI altered the redox conditions in the GB creating a secondary redoxcline at
483 140 m, where the O_2 and the MnOx-like particles concentration increased (Fig. 4a). One
484 consequence of those changes is the vertical extension of the layer in which MnOx aggregates
485 could form. A previous study showed that MnOx might precipitate from the water column of the
486 GB following a MBI event (Lenz et al., 2015). Scavenging of phosphate into Mn or Fe oxides had
487 been shown in previous studies (Neretin et al., 2003). Moreover, Gustafsson and Stigebrandt,
488 2007 showed that there is a downward flux of phosphate, associated with particulate iron and
489 MnOx, from the oxygenated water column to the anoxic deep waters. On the other hand, the
490 intrusion of oxygenated water masses associated with the MBI caused turbulent mixing the deep
491 water of the GB. Myllykangas et al. (2017) reported that following the 2014/2015 MBI, the GB
492 experienced the displacement of stagnant water masses by the new water masses intruded during
493 the MBI. Thus, the low concentrations of silicate and phosphate that we measured in the deep
494 waters of the GB may also be a direct consequence of the intrusion of oxygenated, low-nutrient
495 waters associated with the MBI. In contrast, in the LD, the water column remained suboxic down
496 the sea floor (430 m), below the oxycline an increase of ammonium was observed (Fig.2b) which

497 could be an indicator for anaerobic respiration of OM, e.g., denitrification (Bonaglia et al., 2016;
498 Hietanen et al., 2012).

499 In summary, although the GB and the LD had similar surface conditions in terms of
500 phytoplankton production and POM stocks, during this study, we found differences the vertical
501 concentration of nutrients (Fig. 2) and POM (Fig. 3) in the GB, ventilated by the MBI, relative to
502 the LD, a station that remains suboxic. Our results suggest that physical processes and differences
503 in the vertical profile of O₂ may modify the redox conditions of the water column, enhance the
504 formation of MnOx-like particles (Fig. 4) that may aggregate with POM in the GB (or transported
505 to the GB by the inflow) influencing the vertical distribution of POM in the water column.

506 *4.2 Potential influence of O₂ concentration and redox conditions on sinking fluxes of POM in the* 507 *GB and the LD*

508 During this study, we also investigated the effect of different O₂ concentrations and redox
509 conditions on the fluxes of particles. Our measurement of carbon flux at 40 m, below the euphotic
510 zone, were 11.7±0.82 mmol C m⁻² d⁻¹ in the GB and 19.8±1.22 mmol C m⁻² d⁻¹ in the LD.
511 Extrapolating those measurements to annual flux we obtain 4.37±0.31 mol C m⁻² a⁻¹ in the GB and
512 7.44±0.46 mol C m⁻² a⁻¹ in the LD. Our results from the LD are comparable in the same range
513 that with the long-term annual estimations from models that varied between 3.8 to 4.2 mol C m⁻² d⁻¹
514 ¹ (Kreus and Schartau, 2015; Sandberg et al., 2000; Stigebrandt, 1991) for the Baltic Sea;
515 however, the estimations based on our results from the GB are higher than the C fluxes predicted
516 by those models.

517 The vertical flux of POM was different in the two studied stations. In the GB, the POM fluxes
518 showed distinct trends with depth; while the POC flux slightly decreased from below the upper
519 oxycline (60 m) to 180 m, the PN flux slightly increased with depth. On the other hand, the fluxes
520 of POP, BSi, Chl *a* and TEP showed a distinctive peak in the core of the OMZ (at 110 m). In the
521 LD, the POC flux decreased in the fully oxygenated upper water column (between 40 and 55 m),
522 and remained relatively constant in the OMZ (between 60 and 180 m); PN flux, steadily;

523 decreased with depth. Similar to GB, but smaller, a peak of POP, BSi, Chl *a* and TEP fluxes was
524 observed at 110 m. This high flux of POM at 110 m in both stations coincided with the
525 appearance of dark, star-shaped particles, particularly evident at GB (Fig. 6a, e), but also present
526 in LD, which may correspond to MnOx particles enriched in OM that have been described in the
527 GB and the LD before (Neretin et al., 2003; Pohl et al., 2004). Similar to the vertical distribution
528 on POM in the water column discussed in the section above, differences in POM fluxes between
529 stations are likely associated with the large inflow of oxygen-rich saltwater that displaced the old,
530 stagnant water masses and changed the chemistry of the water column (Myllykangas et al., 2017).
531 Under euxinic (*e.i.*, no MBI) conditions, the maximum concentration of particulate Mn is found at
532 the depth of the oxycline (Glockzin et al., 2014). Below the oxycline, and due to the hydrogen
533 sulfide (H₂S) presence, the particulate Mn concentration decreased drastically. During this study,
534 we observed high concentration of MnOx particles flux at 110 and 180 m (Table 5) in the GB;
535 this result agreed with the high flux of particulate Mn measured in sediment traps located at 186
536 m in June 2015 (Dellwig et al., 2018). The oxygenation of the deep water layers of the GB by the
537 MBI caused the absence of H₂S (Schmale et al., 2016) and provided the redox conditions to
538 measured high MnOx flux in the sediment trap located in the core of the OMZ (110 m) and at 180
539 m. There were two possible sources of MnOx in the GB associated with the 2014/2015 MBI, on
540 one hand, the lateral transport of low-density aggregates formed by MnOx and OM (Glockzin et
541 al., 2014), and on the other hand, the remarkable *in-situ* formation and deposition of MnOx from
542 dissolved Mn, which inventory drastically decreased in the water column due to the change in
543 redox conditions (Dellwig et al., 2018). In clear contrast to the oxygenated deep layers of the GB,
544 in the LD, we measured H₂S at 180 m, this could explain why although those aggregates were
545 present in this station below the oxycline (*i.e.*, 70 m) at 110 m, they dissolved in sulfidic waters,
546 thus were not as abundant, and did not form aggregates with TEP (Fig.6c).

547 The presence of MnOx-containing aggregates enriched in OM (see TEP fluxes, Fig 6c) may have
548 implications for the vertical flux of C and N in a stratified system with a pelagic redoxcline like
549 the Baltic Sea. Under steady state, the upward diffusion and oxidation rate of the dissolved Mn

550 are balanced by the sinking and dissolution rate of MnOx. During the Mn-oxidation, the POM
551 could aggregate with the MnOx including particulate elements, and trace metals. Then, in the
552 sulfidic waters, slow-sinking MnOx enriched in OM will be dissolved liberating the OM and
553 altering the vertical distribution and the flux of all associated particle elements (Glockzin et al.,
554 2014). For example, in the Cariaco Basin, total particulate phosphorus reached their maximum
555 flux in sediment traps close to the redoxcline (Benitez-Nelson et al., 2004; Benitez-Nelson et al.,
556 2007). MnOx formation and scavenging of trace metal may be a relevant mechanism for transfer
557 trace metals from the oxygenated to the anoxic deep waters (Dellwig et al., 2010). Moreover,
558 even in the anoxic zone, the abundant aggregate associated bacteria (Grossart et al., 2006) could
559 partially or completely degrade the organic compounds in those particles using NO₃⁻ or MnOx as
560 an electron acceptor. This may [explain](#) why we observed a clear peak in the flux of POP, BSi, Chl
561 a (Fig. 3a, b), TEP (Fig. 6a) and TCHO (Fig. 7a) at 110 m followed by a small decrease at 180 m
562 in the GB. In the LD a smaller increment in the flux of POP, BSi (Fig. 3d), TEP (Fig. 6c) and
563 TCHO (Fig. 7b) was also observed. The vertical fluxes of those compounds coincided with the
564 abundance of MnOx particles; we assume that the MnOx aggregated not only with TEP as
565 described before (Glockzin et al. 2014) and observed in this study (Fig. 6a) but also with POP,
566 BSi, Chl a, and TCHO. On the other hand, nitrogen-rich [components of POM](#) like PN (Fig. 3a),
567 TAA (Fig. 7a), and CSP (Fig. 6a) gradually decreased with depth in the GB, suggesting that those
568 compounds were less scavenge by MnOx-[OM](#) rich aggregates.

569 Primary production (PP) in the GB was 10% higher than in LD during our study (Piontek et al.
570 unpublished data). However, the POC flux below the euphotic zone (at 40 m) was 42% higher in
571 LD than in GB and comparable at both stations at 180 m. The fraction of PP exported as POC is
572 termed export production (*e-ratio*) (Buesseler et al., 1992), and it is calculated as the POC flux
573 below the euphotic zone divided by the primary production. The *e-ratio* was calculated here using
574 the ¹⁴C based PP (Piontek et al. unpublished data) and carbon flux at 40 m (shallowest sediment
575 trap depth, considered at the base of the euphotic zone). The *e-ratio* was 0.41 in the GB and 0.77
576 in the LD; *i.e.*, in GB 41% of the primary production was exported as POC below the euphotic

577 zone (40 m) versus 77% in the LD. This suggests that a higher proportion of the primary
578 production was remineralized in the euphotic zone of the GB compared with the LD. On the other
579 hand, the transfer efficiency of POC to the deeper water column (*i.e.* the ratio of POC flux at 180
580 m over POC flux at 40 m) was higher in the GB (115%) than in the LD (69%). The transfer
581 efficiency of POM is largely controlled by the remineralization rate and the sinking velocity of
582 particles (De La Rocha and Passow, 2007; McDonnell et al., 2015; Trull et al., 2008). The higher
583 POC transfer efficiency in the GB than in the LD can be attributable to differences in the sinking
584 velocities of the particles in those two stations. Particulate MnOx may sink through the redoxcline
585 in the GB (Neretin et al., 2003) acting as ballast material and nucleus for MnOx-OM rich
586 aggregates formation. Those aggregates could have sunk more quickly, limiting the time spent in
587 the water column and the degradation by particle- attached microbes. Assuming that MnOx had a
588 density between 1.5 and 2.0 g cm⁻³ (Glockzin et al., 2014). The largest particles measured in GB
589 (167 μm, Table 4) will have a sinking velocity based in Stokes' law between 508 and 1014 m d⁻¹.
590 If we considered a mixed aggregate that is 50% TEP, density 0.9 g cm⁻³ (Azetsu-Scott and
591 Passow, 2004) and 50% MnOx (density 1.5 g cm⁻³), its density would be 1.2 g cm⁻³, and its
592 theoretical sinking velocity will be 204 m d⁻¹. This indicates that theoretically, the largest mix
593 aggregates composed of MnOx and TEP observed in the GB could reach 180 m (the location of
594 our deepest sediment trap) in less than one day. However, the average measured sinking velocity
595 of MnOx in the laboratory for particles between 2 and 20 μm was 0.76 m d⁻¹, this is significantly
596 lower than the theoretical value (Glockzin et al., 2014). Glockzin et al. (2014) suggested that the
597 star shape and the content of OM were responsible for the lower than predicted sinking velocity.
598 There is no information about the amount of OM relatively to MnOx particles in those mix
599 aggregates, or how the MnOx to OM ratio may affect the density and sinking velocity of larger
600 aggregates like the ones we observed. Due to the shape and size of MnOx-OM aggregates
601 observed in our study (Fig. 6e), we could assume those are the same type of aggregates described
602 before by Glockzin et al. (2014). Although we did not measure the sinking velocity of those
603 aggregates, we did observe a higher abundance of them associated with TEP at 110 and 180 m in

604 the GB than in the LD. The formation of these organic matter rich MnOx aggregates could
605 represent an additional mechanism (see introduction) to explain why the efficiency of the OM
606 export is different under anoxic than under oxic conditions in the Baltic Sea. The oxygenation of
607 anoxic deep water in the GB caused by the 2014/2015 MBI, may have led to an enhanced
608 precipitation of manganese, iron and phosphorus particles (Dellwig et al., 2010; Dellwig et al.,
609 2018). For example, the formation of P-rich, metal oxides precipitates occur in the anoxic waters
610 of the Black Sea (Shaffer, 1986) and Cariaco Basin (Benitez-Nelson et al., 2004; Benitez-Nelson
611 et al., 2007) where higher concentration of particulate inorganic and organic phosphorus have been
612 observed in sediment traps close to the redoxcline.

613 *4.3 Differences on composition and lability of sinking and suspended organic matter in the GB* 614 *and the LD*

615 In the sections above, we discussed how similar were biogeochemical conditions and the size of
616 the surface POM pool in both the GB and the LD. We then looked at how the sinking flux of OM
617 was affected by the different O₂ concentrations in the water column. We now focus on the
618 influence of O₂ in the chemical composition of sinking and suspended POM. Suspended or slow
619 sinking POM, that spend more time in the water column, should theoretically, show a larger
620 degree of degradation (Goutx et al., 2007). Relative to the Redfield molar ratio: 106 POC:16
621 PN:POP, OM showed an enrichment in carbon, especially in sinking particles from the LD and
622 suspended OM from the GB (Table 5). Our measured values of POC:PN (~10) and POC:POP
623 (between 89 and 506) in suspended OM coincide with the simulated ratio reported by Kreuz et al.
624 (2015) immediately after the culmination of the spring bloom, those relatively high ratios are
625 consequence of the nitrogen depletion and are characteristic during the summer in the Baltic Sea.
626 The same study had suggested that POC:POP higher than Redfield ratio might lead to an
627 enhancement of particle export (Kreuz et al., 2015), however, no direct observations had
628 confirmed this hypothesis. Our measurements showed that the relative higher POC:POP ratios in
629 sinking OM from LD, compared with the GB, do not lead to a higher transfer efficiency at this

630 station. Compared to the suspended OM in the LD, the POP content was lower in the GB,
631 possible related to scavenging of POP into MnOx aggregates (see section 3.4).

632 The TAA based degradation index, DI (Dauwe et al. 1999) covers a wide range of alteration
633 stages; the more negative the DI, the more degraded the samples, positive DI indicates fresh
634 organic matter. In our study, the sediment trap material had a DI between 0.10 and 1.14, while
635 suspended OM has a DI between -0.26 and -1.25 (Table 4). These values coincide with what
636 reported earlier by Dauwe et al. (1999), and indicate that: first, the sinking particles collected in
637 the sediment traps were less altered (they have a more positive DI) than the suspended OM
638 collected in the [Niskin bottle](#). Second, sinking particles from the GB were fresher than the ones
639 from the LD, and the degradation stage increased with depth in both stations. The higher
640 contribution of AA and CHO to the POC pool in sinking than in suspended OM and the AA- DI
641 indicates that suspended OM was more degraded than sinking OM. The highest degree of
642 degradation in suspended OM and sinking OM from the LD may be the result of a long time that
643 light suspended OM or slow sinking particles spend exposed to degradation in fully oxygenated
644 surface waters than dense, fast sinking particles collected in sediment traps.

645 The higher abundance of aggregates, formed by a combination of MnOx-like particles and OM,
646 observed at 110 and 180 m in the GB could act as bacteria hot spots that combined with a higher
647 O₂ concentration in the GB may increase the microbial degradation on sinking particles collected
648 in the GB. However, the AA-DI, indicated that sinking OM was less altered and therefore more
649 labile than the sinking OM in the LD. This implied that in addition to the higher transfer
650 efficiency of POC in the GB (see discussion above); the OM reaching the seafloor was fresher
651 and less degraded. This supports the idea that mix aggregates composed by MnOx and OM may
652 be larger and faster sinking than the previously described by Glockzin et al. (2014). This
653 explanation is mostly speculative, and based on the observation of large mixed aggregates in the
654 110 and 180 m traps (Fig. 6, Table 4). However, as mention in the previous section, further work
655 on directly determines sinking velocity is required to prove this hypothesis.

656 **Conclusion**

657 Fluxes and composition of sinking particles were different in two deep basins in the Baltic Sea:
658 the GB and the LD during early summer 2015. The two stations had similar surface characteristics
659 and POM stock; however, at depth, the vertical profile of the O₂ concentration was different. The
660 2014/2015 MBI supplied oxygen-rich waters to the GB transporting solid material from the and
661 modifying the O₂ vertical profile and the redox conditions in the otherwise permanent suboxic
662 deep waters. This event did not affect the LD allowing the comparing POM fluxes and
663 composition under two different O₂ concentrations with similar surface water conditions. Export
664 efficiency (*e-ratio*) derived from *in-situ* PP measurements and POC flux derivate from sediment
665 traps indicated higher export efficiency in LD than in GB. However, the transfer efficiency (POC
666 flux at 180 m over POC flux at 40 m) suggested that under anoxic conditions found in the LD, a
667 smaller portion of the POC exported below the euphotic zone was transferred to 180 m than under
668 re-oxygenated conditions present in the GB. The 2014/2015 MBI also transport solid Mn from
669 shallower areas towards the GB deep that may have contributed to the higher abundance of
670 MnOx-OM in the GB. Our results suggest that a new possible mechanism to explain the
671 differences in the OM fluxes under different O₂ concentration could be the formation and
672 prevalence of aggregates composed of MnOx and organic matter in the GB. Those aggregates
673 were significantly larger and more abundant in the GB compared to the LD where sulfidic waters
674 constrained their presence. We propose that after a MBI in the GB, the aggregates containing
675 MnOx-like particles and organic matter could have reached the sediments relatively fast and
676 unaltered, scavenging not only phosphorus and TEP, as described previously, but also other
677 organic compounds. The remineralization of this organic matter reaching the sediments may
678 contribute to the quick re-establishment of anoxic conditions in the sediment-water interface in
679 the GB. The relevance of this process needs s to be further investigated d in order to be included in
680 O₂ budget and long-term predictions of the MBI impact in the O₂ and OM cycles.

681 **Author Contributions**

682 C.C.N. performed deployments, analyzed samples and wrote the manuscript. F.A.C.L.M.,
683 performed deployments and contributed to the writing of the manuscript. A.E designed and
684 conducted the scientific program at sea and discussed and commented on the manuscript.

685 **Acknowledgements**

686 This research was supported by the DFG Collaborative Research Center 754 “Climate-
687 Biogeochemistry Interactions in the Tropical Ocean” (to A.E., C.C.N. and F.A.C.L.M), by a
688 Fellowship of the Excellence Cluster ‘The Future Ocean’ (CP1403 to F.A.C.L.M.), and by a
689 DAAD short term grant (57130097 to C.C.N.). We thank Jon Roa, Tania Klüver, Scarlett Sett,
690 Angela Stippkugel, Carola Wagner, Clarissa Karthäuser, Moritz Ehrlich, Sonja Endres, Hannes
691 Wagner, Ruth Flerus, Sven Sturm and Christian Begler for support during traps preparation and
692 deployments, help with experiment or analyzed samples. We Thank Judith Piontek for her
693 contribution to the design of the scientific program at sea, Jaime Soto- Neira for useful discussion
694 and help with figure preparation and Cindy Lee for helpful advices.

References

- Aldredge, A. L., Passow, U., and Logan, B. E.: The abundance and significance of a class of large, transparent organic particles in the ocean, *Deep Sea Research Part I: Oceanographic Research Papers*, 40, 1131-1140, 1993.
- Andersen, J. H., Carstensen, J., Conley, D. J., Dromph, K., Fleming-Lehtinen, V., Gustafsson, B. G., Josefson, A. B., Norkko, A., Villnäs, A., and Murray, C.: Long-term temporal and spatial trends in eutrophication status of the Baltic Sea, *Biological Reviews*, 92, 135-149, 2017.
- Armstrong, R. A., Lee, C., Hedges, J. I., Honjo, S., and Wakeham, S. G.: A new, mechanistic model for organic carbon fluxes in the ocean based on the quantitative association of POC with ballast minerals, *Deep Sea Research Part II: Topical Studies in Oceanography*, 49, 219-236, 2002.
- Azetsu-Scott, K. and Passow, U.: Ascending marine particles: Significance of transparent exopolymer particles (TEP) in the upper ocean, *Limnology and Oceanography*, 49, 741-748, 2004.
- Benitez-Nelson, C. R., O'Neill, L., Kolowitz, L. C., Pellechia, P., and Thunell, I. R.: Phosphonates and particulate organic phosphorus cycling in an anoxic marine basin, *Limnology and Oceanography*, 49, 1593-1604, 2004.
- Benitez-Nelson, C. R., O'Neill Madden, L. P., Styles, R. M., Thunell, R. C., and Astor, Y.: Inorganic and organic sinking particulate phosphorus fluxes across the oxic/anoxic water column of Cariaco Basin, Venezuela, *Marine Chemistry*, 105, 90-100, 2007.
- Bianchi, T. S., Engelhaupt, E., Westman, P., Andrén, T., Rolff, C., and Elmgren, R.: Cyanobacterial blooms in the Baltic Sea: Natural or human-induced?, *Limnology and Oceanography*, 45, 716-726, 2000.
- Bonaglia, S., Klawonn, I., Brabandere, L. D., Deutsch, B., Thamdrup, B., and Brüchert, V.: Denitrification and DNRA at the Baltic Sea oxic–anoxic interface: Substrate spectrum and kinetics, *Limnology and Oceanography*, 61, 1900-1915, 2016.
- Boyd, P. W. and Trull, T. W.: Understanding the export of biogenic particles in oceanic waters: Is there consensus?, *Progress in Oceanography*, 72, 276-312, 2007.
- Brettar, I. and Rheinheimer, G.: Denitrification in the Central Baltic: evidence for H₂S-oxidation as motor of denitrification at the oxic-anoxic interface, *Marine Ecology Progress Series*, 77, 157-169, 1991.
- Buesseler, K. O., Bacon, M. P., Kirk Cochran, J., and Livingston, H. D.: Carbon and nitrogen export during the JGOFS North Atlantic Bloom experiment estimated from ²³⁴Th: ²³⁸U disequilibria, *Deep Sea Research Part A. Oceanographic Research Papers*, 39, 1115-1137, 1992.
- Carstensen, J., Andersen, J. H., Gustafsson, B. G., and Conley, D. J.: Deoxygenation of the Baltic Sea during the last century, *Proceedings of the National Academy of Sciences*, 111, 5628-5633, 2014a.
- Carstensen, J., Conley, D. J., Bonsdorff, E., Gustafsson, B. G., Hietanen, S., Janas, U., Jilbert, T., Maximov, A., Norkko, A., Norkko, J., Reed, D. C., Slomp, C. P., Timmermann, K., and Voss, M.: Hypoxia in the Baltic Sea: Biogeochemical Cycles, Benthic Fauna, and Management, *AMBIO*, 43, 26-36, 2014b.
- Cavan, E. L., Trimmer, M., Shelley, F., and Sanders, R.: Remineralization of particulate organic carbon in an ocean oxygen minimum zone, *Nature Communications*, 8, 14847, 2017.
- Cisternas-Novoa, C., Lee, C., and Engel, A.: A semi-quantitative spectrophotometric, dye-binding assay for determination of Coomassie Blue stainable particles, *Limnology and Oceanography: Methods*, 12, 604-616, 2014.
- Conley, D. J., Björck, S., Bonsdorff, E., Carstensen, J., Destouni, G., Gustafsson, B. G., Hietanen, S., Kortekaas, M., Kuosa, H., Markus Meier, H. E., Müller-Karulis, B., Nordberg, K., Norkko, A., Nürnberg, G., Pitkänen, H., Rabalais, N. N., Rosenberg, R., Savchuk, O. P., Slomp, C. P., Voss, M., Wulff, F., and Zillén, L.: Hypoxia-Related Processes in the Baltic Sea, *Environmental Science & Technology*, 43, 3412-3420, 2009.
- Dauwe, B., Middelburg, J. J., Herman, P. M. J., and Heip, C. H. R.: Linking diagenetic alteration of amino acids and bulk organic matter reactivity, *Limnology and Oceanography*, 44, 1809-1814, 1999.

De La Rocha, C. L. and Passow, U.: Factors influencing the sinking of POC and the efficiency of the biological carbon pump, *Deep Sea Research Part II: Topical Studies in Oceanography*, 54, 639-658, 2007.

Dellwig, O., Leipe, T., März, C., Glockzin, M., Pollehne, F., Schnetger, B., Yakushev, E. V., Böttcher, M. E., and Brumsack, H.-J.: A new particulate Mn–Fe–P-shuttle at the redoxcline of anoxic basins, *Geochimica et Cosmochimica Acta*, 74, 7100-7115, 2010.

Dellwig, O., Schnetger, B., Meyer, D., Pollehne, F., Häusler, K., and Arz, H. W.: Impact of the Major Baltic Inflow in 2014 on Manganese Cycling in the Gotland Deep (Baltic Sea), *Frontiers in Marine Science*, 5, 2018.

Devol, A. H. and Hartnett, H. E.: Role of the oxygen-deficient zone in transfer of organic carbon to the deep ocean, *Limnology and Oceanography*, 46, 1684-1690, 2001.

Dittmar, T., Cherrier, J., and Ludwichowski, K. U.: The analysis of amino acids in seawater. In: *Practical guidelines for the analysis of seawater* Wurl, O. and Raton, B. (Eds.), CRC Press, 2009.

Dollhopf, M. E., Nealson, K. H., Simon, D. M., and Luther, G. W.: Kinetics of Fe(III) and Mn(IV) reduction by the Black Sea strain of *Shewanella putrefaciens* using in situ solid state voltammetric Au/Hg electrodes, *Marine Chemistry*, 70, 171-180, 2000.

Dugdale, R. C. and Goering, J. J.: Uptake Of New And Regenerated Forms Of Nitrogen In Primary Productivity, *Limnology and Oceanography*, 12, 196-206, 1967.

Emeis, K. C., Struck, U., Leipe, T., Pollehne, F., Kunzendorf, H., and Christiansen, C.: Changes in the C, N, P burial rates in some Baltic Sea sediments over the last 150 years—relevance to P regeneration rates and the phosphorus cycle, *Marine Geology*, 167, 43-59, 2000.

Engel, A.: The role of transparent exopolymer particles (TEP) in the increase in apparent particle stickiness (α) during the decline of a diatom bloom, *Journal of Plankton Research*, 22, 485-497, 2000.

Engel, A., Meyerhöfer, M., and von Bröckel, K.: Chemical and Biological Composition of Suspended Particles and Aggregates in the Baltic Sea in Summer (1999), *Estuarine, Coastal and Shelf Science*, 55, 729-741, 2002.

Engel, A. and Schartau, M.: Influence of transparent exopolymer particles (TEP) on sinking velocity of *Nitzschia closterium* aggregates, *Marine Ecology Progress Series*, 182, 69-76, 1999.

Engel, A., Wagner, H., Le Moigne, F. A. C., and Wilson, S. T.: Particle export fluxes to the oxygen minimum zone of the eastern tropical North Atlantic, *Biogeosciences*, 14, 1825-1838, 2017.

Eppley, R. W. and Peterson, B. J.: Particulate organic matter flux and planktonic new production in the deep ocean, *Nature*, 282, 677, 1979.

Glockzin, M., Pollehne, F., and Dellwig, O.: Stationary sinking velocity of authigenic manganese oxides at pelagic redoxclines, *Marine Chemistry*, 160, 67-74, 2014.

Goutx, M., Wakeham, S. G., Lee, C., Duflo, s. M., Guigue, C., Liu, Z., Moriceau, B., Sempère, R., Tedetti, M., and Xue, J.: Composition and degradation of marine particles with different settling velocities in the northwestern Mediterranean Sea, *Limnology and Oceanography*, 52, 1645-1664, 2007.

Grossart, H. P., KiÅfÅrboe, T., Tang, K. W., Allgaier, M., Yam, E. M., and Ploug, H.: Interactions between marine snow and heterotrophic bacteria: aggregate formation and microbial dynamics, *Aquatic Microbial Ecology*, 42, 19-26, 2006.

Günter, J., Zubkov, M. V., Yakushev, E., Labrenz, M., and Jürgens, K.: High abundance and dark CO₂ fixation of chemolithoautotrophic prokaryotes in anoxic waters of the Baltic Sea, *Limnology and Oceanography*, 53, 14-22, 2008.

Gustafsson, B. G. and Stigebrandt, A.: Dynamics of nutrients and oxygen/hydrogen sulfide in the Baltic Sea deep water, *Journal of Geophysical Research: Biogeosciences*, 112, 2007.

Hannig, M., Lavik, G., Kuypers, M. M. M., Woebken, D., Martens-Habbena, W., and Jürgens, K.: Shift from denitrification to anammox after inflow events in the central Baltic Sea, *Limnology and Oceanography*, 52, 1336-1345, 2007.

Hansen, H. P. and Koroleff, F.: Determination of nutrients. In: *Methods of Seawater Analysis*., Grasshoff, K., Kremling, K., and Ehrhardt, M. (Eds.), Wiley-VCH, Weinheim, Germany, 1999.

Hansen, H. P. and Koroleff, F.: Determination of nutrients. In: *Methods of Seawater Analysis*, Wiley-VCH Verlag GmbH, 2007.

Hietanen, S., Jäntti, H., Buizert, C., Jürgens, K., Labrenz, M., Voss, M., and Kuparinen, J.: Hypoxia and nitrogen processing in the Baltic Sea water column, *Limnology and Oceanography*, 57, 325-337, 2012.

Holtermann, P. L., Prien, R., Naumann, M., Mohrholz, V., and Umlauf, L.: Deepwater dynamics and mixing processes during a major inflow event in the central Baltic Sea, *Journal of Geophysical Research: Oceans*, 122, 6648-6667, 2017.

Keil, R. G., Neibauer, J. A., Biladeau, C., van der Elst, K., and Devol, A. H.: A multiproxy approach to understanding the "enhanced" flux of organic matter through the oxygen-deficient waters of the Arabian Sea, *Biogeosciences*, 13, 2077-2092, 2016.

Knauer, G. A., Martin, J. H., and Bruland, K. W.: Fluxes of particulate carbon, nitrogen, and phosphorus in the upper water column of the northeast Pacific, *Deep Sea Research Part A. Oceanographic Research Papers*, 26, 97-108, 1979.

Kreus, M. and Schartau, M.: Variations in the elemental ratio of organic matter in the central Baltic Sea: Part II – Sensitivities of annual mass flux estimates to model parameter variations, *Continental Shelf Research*, 100, 46-63, 2015.

Kreus, M., Schartau, M., Engel, A., Nausch, M., and Voss, M.: Variations in the elemental ratio of organic matter in the central Baltic Sea: Part I—Linking primary production to remineralization, *Continental Shelf Research*, 100, 25-45, 2015.

Kullenberg, G. and Jacobsen, T. S.: The Baltic Sea: an outline of its physical oceanography, *Marine Pollution Bulletin*, 12, 183-186, 1981.

Le Moigne, F. A. C., Cisternas-Novoa, C., Piontek, J., Maßmig, M., and Engel, A.: On the effect of low oxygen concentrations on bacterial degradation of sinking particles, *Scientific Reports*, 7, 16722, 2017.

Legendre, L. and Gosselin, M.: New production and export of organic matter to the deep ocean: Consequences of some recent discoveries, *Limnology and Oceanography*, 34, 1374-1380, 1989.

Leipe, T., Tauber, F., Vallius, H., Virtasalo, J., Uścińowicz, S., Kowalski, N., Hille, S., Lindgren, S., and Myllyvirta, T.: Particulate organic carbon (POC) in surface sediments of the Baltic Sea, *Geo-Marine Letters*, 31, 175-188, 2011.

Lenz, C., Jilbert, T., Conley, D. J., Wolthers, M., and Slomp, C. P.: Are recent changes in sediment manganese sequestration in the euxinic basins of the Baltic Sea linked to the expansion of hypoxia?, *Biogeosciences*, 12, 4875-4894, 2015.

Lindroth, P. and Mopper, K.: High performance liquid chromatographic determination of subpicomole amounts of amino acids by precolumn fluorescence derivatization with o-phthalaldehyde, *Analytical Chemistry*, 51, 1667-1674, 1979.

Logan, B. E., Passow, U., Alldredge, A. L., Grossartt, H.-P., and Simont, M.: Rapid formation and sedimentation of large aggregates is predictable from coagulation rates (half-lives) of transparent exopolymer particles (TEP), *Deep Sea Research Part II: Topical Studies in Oceanography*, 42, 203-214, 1995.

Long, R. A. and Azam, F.: Abundant protein-containing particles in the sea, *Aquatic Microbial Ecology*, 10, 213-221, 1996.

Mari, X. and Burd, A.: Seasonal size spectra of transparent exopolymeric particles (TEP) in a coastal sea and comparison with those predicted using coagulation theory, *Marine Ecology Progress Series*, 163, 13, 1998.

Mari, X., Passow, U., Migon, C., Burd, A. B., and Legendre, L.: Transparent exopolymer particles: Effects on carbon cycling in the ocean, *Progress in Oceanography*, 151, 13-37, 2017.

Mari, X., Rassoulzadegan, F., Brussaard, C. P. D., and Wassmann, P.: Dynamics of transparent exopolymeric particles (TEP) production by *Phaeocystis globosa* under N- or P-limitation: a controlling factor of the retention/export balance, *Harmful Algae*, 4, 895-914, 2005.

McDonnell, A. M. P., Boyd, P. W., and Buesseler, K. O.: Effects of sinking velocities and microbial respiration rates on the attenuation of particulate carbon fluxes through the mesopelagic zone, *Global Biogeochemical Cycles*, 29, 175-193, 2015.

Myllykangas, J. P., Jilbert, T., Jakobs, G., Rehder, G., Werner, J., and Hietanen, S.: Effects of the 2014 major Baltic inflow on methane and nitrous oxide dynamics in the water column of the central Baltic Sea, *Earth Syst. Dynam.*, 8, 817-826, 2017.

Nausch, M., Nausch, G., Lass, H. U., Mohrholz, V., Nagel, K., Siegel, H., and Wasmund, N.: Phosphorus input by upwelling in the eastern Gotland Basin (Baltic Sea) in summer and its effects on filamentous cyanobacteria, *Estuarine, Coastal and Shelf Science*, 83, 434-442, 2009.

Neretin, L. N., Pohl, C., Jost, G., Leipe, T., and Pollehne, F.: Manganese cycling in the Gotland Deep, Baltic Sea, *Marine Chemistry*, 82, 125-143, 2003.

Passow, U.: Production of transparent exopolymer particles (TEP) by phyto- and bacterioplankton, *Marine Ecology Progress Series*, 236, 12, 2002.

Passow, U. and Alldredge, A. L.: A dye-binding assay for the spectrophotometric measurement of transparent exopolymer particles (TEP), *Limnology and Oceanography*, 40, 1326-1335, 1995.

Pohl, C., Löffler, A., and Hennings, U.: A sediment trap flux study for trace metals under seasonal aspects in the stratified Baltic Sea (Gotland Basin; 57°19.20'N; 20°03.00'E), *Marine Chemistry*, 84, 143-160, 2004.

Richardson, L. L., Aguilar, C., and Neelson, K. H.: Manganese oxidation in pH and O₂ microenvironments produced by phytoplankton^{1,2}, *Limnology and Oceanography*, 33, 352-363, 1988.

Sandberg, J., Elmgren, R., and Wulff, F.: Carbon flows in Baltic Sea food webs — a re-evaluation using a mass balance approach, *Journal of Marine Systems*, 25, 249-260, 2000.

Schmale, O., Krause, S., Holtermann, P., Power Guerra, N. C., and Umlauf, L.: Dense bottom gravity currents and their impact on pelagic methanotrophy at oxic/anoxic transition zones, *Geophysical Research Letters*, 43, 5225-5232, 2016.

Shaffer, G.: Phosphate pumps and shuttles in the Black Sea, *Nature*, 321, 515, 1986.

Stigebrandt, A.: Computations of oxygen fluxes through the sea surface and the net production of organic matter with application to the Baltic and adjacent seas, *Limnology and Oceanography*, 36, 444-454, 1991.

Strickland, J. D. and Parsons, T. R.: Determination of dissolved oxygen. In: *A Practical Handbook of Seawater Analysis*, Fisheries Research Board of Canada, 1968.

Strickland, J. D. H., Parsons, T. R., and Strickland, J. D. H.: *A practical handbook of seawater analysis*, Fisheries Research Board of Canada, Ottawa, 1972.

Thomas, H. and Schneider, B.: The seasonal cycle of carbon dioxide in Baltic Sea surface waters, *Journal of Marine Systems*, 22, 53-67, 1999.

Trull, T. W., Bray, S. G., Buesseler, K. O., Lamborg, C. H., Manganini, S., Moy, C., and Valdes, J.: In situ measurement of mesopelagic particle sinking rates and the control of carbon transfer to the ocean interior during the Vertical Flux in the Global Ocean (VERTIGO) voyages in the North Pacific, *Deep Sea Research Part II: Topical Studies in Oceanography*, 55, 1684-1695, 2008.

Turner, J. T.: Zooplankton fecal pellets, marine snow, phytodetritus and the ocean's biological pump, *Progress in Oceanography*, 130, 205-248, 2015.

van Mooy, B. A. S., Keil, R. G., and Devol, A. H.: Impact of suboxia on sinking particulate organic carbon: Enhanced carbon flux and preferential degradation of amino acids via denitrification, *Geochimica et Cosmochimica Acta*, 66, 457-465, 2002.

Wasmund, N.: Occurrence of cyanobacterial blooms in the Baltic Sea in relation to environmental conditions, *Internationale Revue der gesamten Hydrobiologie und Hydrographie*, 82, 169-184, 1997.

Wasmund, N. and Uhlig, S.: Phytoplankton trends in the Baltic Sea, *ICES Journal of Marine Science*, 60, 2003.

Wilhelm, W. L.: Die Bestimmung des im Wasser gelösten Sauerstoffes, *Berichte der deutschen chemischen Gesellschaft*, 21, 2843-2854, 1888.

Figure Captions

Figure 1. Monthly averaged Chl *a* distribution derived from VIIRS for June 2015 in the Baltic Sea. Black circle and “x” indicate the position of the trap deployment and the seawater collection respectively in Gotland Deep (GB) and Landsort Deep (LD). The lower panel shows the trajectory of the trap deployed at GB and LD.

Figure 2. Water column profiles at the location of the sediment trap deployments in (A) the GB, and (B) the LD. Left panel: oxygen (blue), temperature (red), and salinity (black). Middle panel: nitrate (NO_3), nitrite (NO_2), and ammonium (NH_4). Right panel: phosphate (PO_4), and silicate ($\text{Si}(\text{OH})_4$). Grey lines indicate the depths at which we deployed sediment traps.

Figure 3. Particulate organic matter profiles in the water column at the location of the sediment traps deployments in the GB (A, B and C) and the LD (D, E and F). (A and D) particulate organic carbon (POC), particulate nitrogen (PN), and particulate organic phosphorus (POP). (B and E) chlorophyll *a* (Chl *a*) and biogenic silicate (BSi). (C and F) transparent exopolymeric particles (TEP) and Coomassie stainable particles (CSP). Grey lines as figure 2.

Figure 4. MnOx-like containing particles and O_2 concentration profiles in the water column at the location of the sediment traps deployments. (A) the GB and (B) the LD. Grey lines as in figure 3.

Figure 5. Particulate organic matter fluxes in the GB (A and B) and the LD (C and D). (A and C) POC, PN and O_2 (B and D) POP, Chl *a*, and BSi.

Figure 6. TEP and CSP fluxes in the GB (A and B) and the LD (C and D). In addition to the vertical distribution of the flux, each profile is complemented with images captured under the microscope (200x) at each depth. Star-shaped MnOx-like particles are clearly visible in the GB associated to TEP (A), but not with CSP (B). MnOx-like particles were significantly less abundant in the LD (C and D). (F) A larger magnification (400x) image of MnOx-like particles at 110 m showing more detail on the shape of those particles and aggregates formed with TEP.

Figure 7. Total hydrolyzable amino acids (TAA) and total carbohydrates (TCHO) fluxes in (A) the GB, and (B) the LD.

Table 1. Sediment traps deployment and recovery locations, dates, collection times and depths.

Station	Lat	Lon	Date	Station depth	Deployment time (d)	Trap depths (m)
Gotland Basin (GB)	57.21 °N	20.03 °E	08/06/2015	248 m	2	40A, 40B, 60, 110, and 180m
	57.27 °N	20.25 °E	10/06/2015			
Landsort Deep (LD)	58.69 °N	18.55 °E	15/06/2015	460 m	1	40A, 40B, 55, 110, and 180m
	58.68 °N	18.68 °E	16/06/2015			

Table 2. Abundance of chlorophyll and phycoerythrin containing pico- and nanoplankton measured by flow-cytometry in the GB and the LD.

	Depth (m)	Phytoplankton (<u>cells</u> mL ⁻¹)			Cyanobacteria-like (<u>cells</u> mL ⁻¹)		
		picoplankton	nanoplankton	Total	picoplankton	nanoplankton	Total
GB	1	87963	2097	90060	5225	731	5956
	10	94369	2628	96997	8795	920	9716
	40	4999	68	5067	2174	69	2243
	60	4125	35	4160	1990	42	2032
	80	599	7	606	238	15	253
	110	594	7	601	326	29	356
	140	1144	14	1158	356	2	358
	180	908	9	917	366	20	385
	220	2270	19	2289	1063	34	1097
LD	1	92359	2283	94642	834	177	1011
	10	86426	1708	88134	2990	232	3223
	40	2022	92	2114	2243	69	2312
	60	1524	62	1586	1294	24	1318
	70	908	43	951	613	17	630
	110	1735	82	1817	1181	17	1198
	180	1339	75	1415	946	34	980
	250	1593	82	1676	949	36	985
	300	1521	48	1569	1047	17	1064
	350	1608	57	1665	908	12	920
	400	1548	73	1621	1047	22	1069
	430	1562	68	1631	875	19	894

Table 3. Phytoplankton abundances analyzed microscopically in the GB and the LD, volume analyzed was 50 ml per sample.

		GB (cells mL ⁻¹)				LD (cells mL ⁻¹)			
		1 m	10 m	40 m	Total	1 m	10 m	40 m	Total
Cyanophyceae *	Total	14148	13536	0	27684	37368	32526	96	69990
Chryptophyta	Total	140	112	28	280	1400	882	56	2338
Bacillariophyceae	Total	96	94	44	234	462	112	102	676
	<i>Chaetoceros</i> sp.	58	42	24	124	434	106	26	566
	<i>Skeletonema</i> sp.	26	8	12	46	12	0	8	20
	<i>Thalassiosira</i> sp.	12	44	8	64	16	6	68	90
Dinophyceae	Total	3772	4424	1192	9388	9032	7662	1404	18098
	<i>Dinophysis</i> sp.	678	742	2	1422	450	214	4	668
	other	3094	3682	1190	7966	8582	7448	1400	17430
Chlorophyta	Total	5320	6860	28	12208	2072	1022	238	3332
	<i>Planctonema</i> sp.	5320	6860	28	12208	2072	1022	238	3332

* >90% were filamentous cyanobacteria *Aphanizomenon* sp.

Table 4. MnOx-like particles fluxes and size determined by image analysis in GB -and LD.

Station	Depth (m)	MnOx-like particles ($\text{cm}^2 \text{m}^{-2} \text{d}^{-1}$)	Median size ESD (μm)	Size range ESD (μm)
GB	110	5666.1 \pm 993.5	2.8	0.6-166.7
	180	7789.1 \pm 954.7	3.3	0.6-152.7
LD	110	50.3 \pm 1.8	1.8	0.6-16.5
	180	2.6 \pm 0.3	1.4	1.2-9.3

Table 5. Amino acids (AA), carbohydrates (CHO) and elemental molar ratios of sinking and suspended OM in the GB and in the LD.

	Depth (m)	AA-C:POC %	CHO-C:POC %	POC:PN	POC:POP	POC:Bsi	PN:POP
GB	40	19.19	18.26	9.80	244.05	3.86	0.39
sinking OM	40	17.58	17.21	9.43	222.42	4.07	0.43
	60	15.78	17.56	9.52	231.56	2.78	0.29
	110	13.87	22.24	11.31	90.12	1.73	0.15
	180	11.13	18.47	12.68	122.87	2.97	0.23
LD	40	13.52	9.43	12.17	771.70	3.58	0.29
sinking OM	40	14.27	8.40	11.09	413.14	4.12	0.37
	55	19.10	10.97	12.43	331.81	3.03	0.24
	110	13.37	11.97	15.44	229.70	2.67	0.17
	180	14.32	12.85	15.29	341.33	4.19	0.27
GB	1	8.22	16.94	10.39	154.56	91.45	14.88
suspended OM	10	10.81	8.84	10.48	150.51	87.15	14.36
	40	4.91	2.80	9.19	88.78	133.75	9.66
	60	5.43	2.66	9.78	127.36	125.24	13.02
	80	4.67		10.43	144.92		13.89
	110	9.01	6.63	8.45	245.26		29.01
	140	5.34		10.60	283.42		26.73
	180	5.73	4.29	11.37	506.21		44.54
	220	8.57	3.35	12.06	270.78		22.45
LD	1	6.96		8.66	205.29	514.94	23.71
suspended OM	10	12.97	9.12	8.43	196.44	100.91	23.31
	40	0.00	8.88	8.09	335.66	24.48	41.51
	60	6.09	10.26	7.83	300.75	16.89	38.43
	70	7.92	10.72	7.71	291.81	247.80	37.86
	110	12.22	5.41	7.93	224.56		28.32
	180	10.12	11.32	7.02	205.33		29.23
	250	11.97	8.81	6.52	249.36		38.22
	300	10.88		6.71	136.67		20.37
	350	10.67	10.12	6.76	145.80		21.56
	400	9.99		6.18	229.53		37.16
	430	9.35	9.45	7.82	148.61		19.01

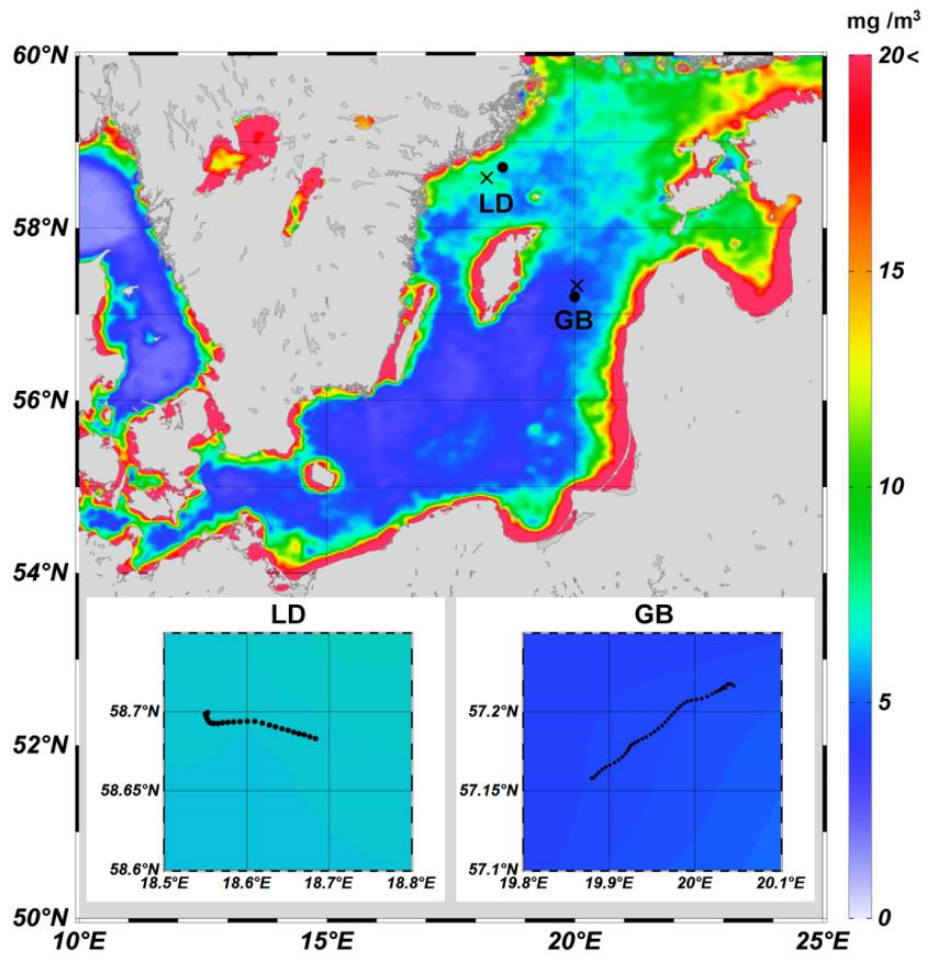


Fig. 1

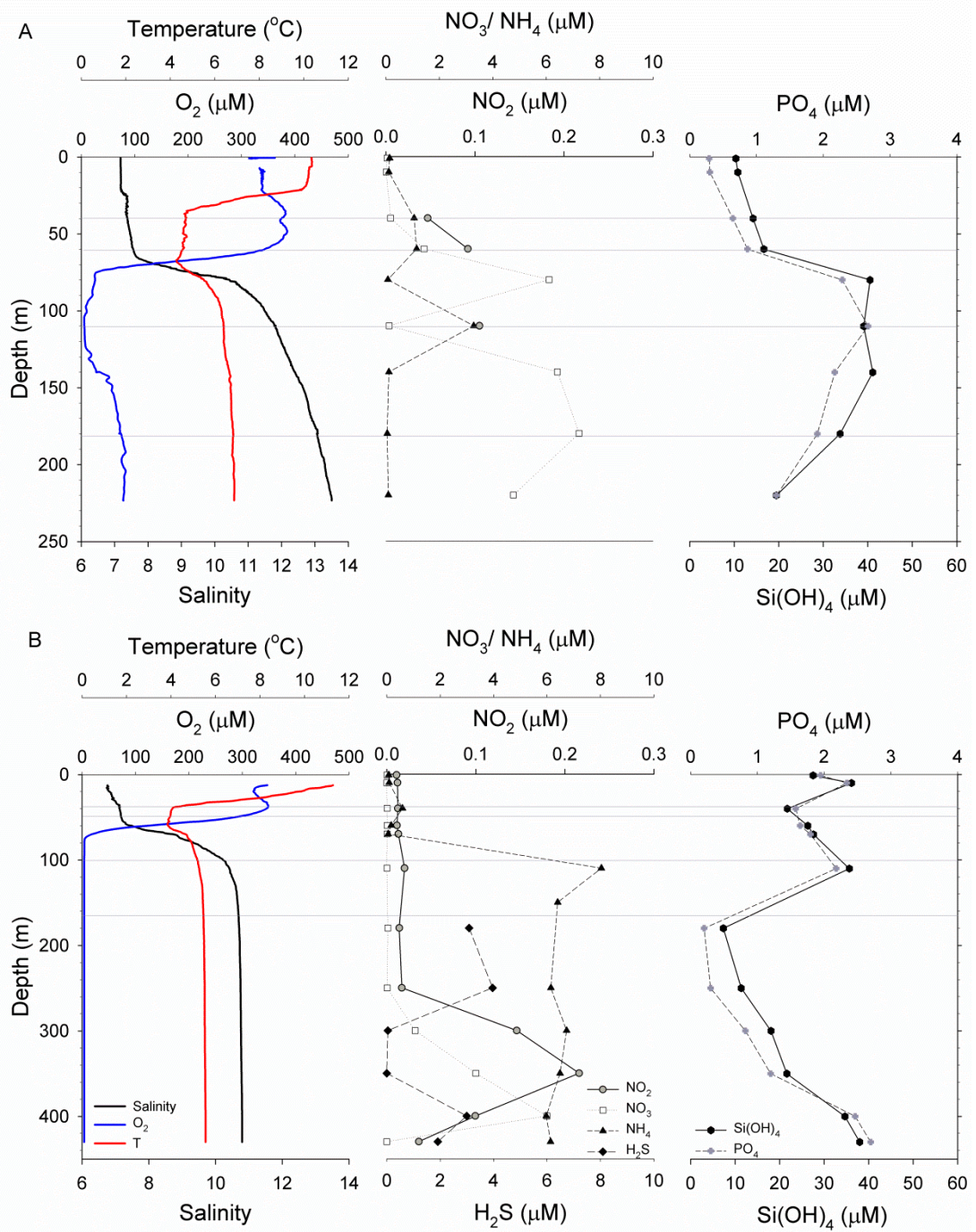


Fig. 2

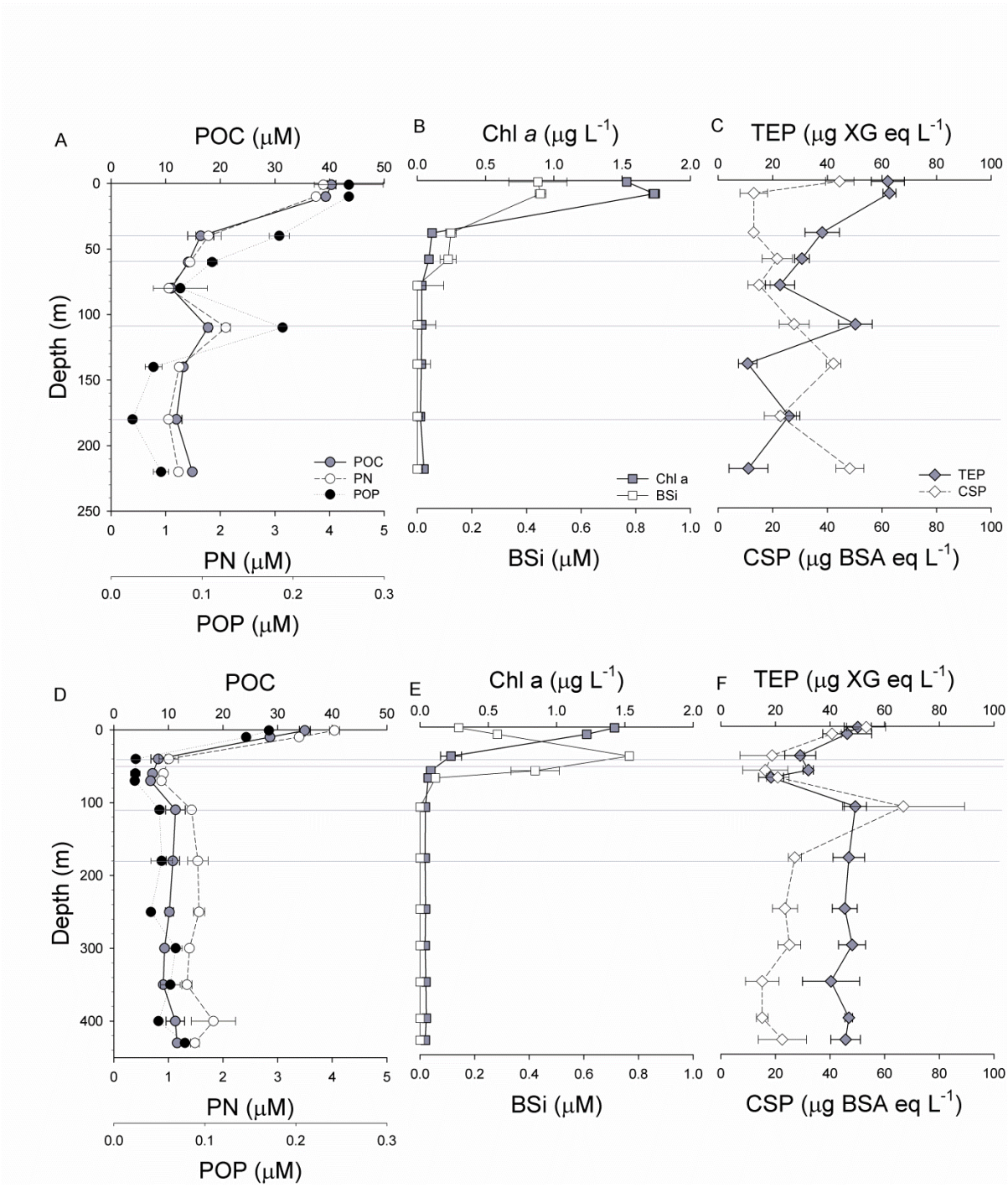


Fig. 3

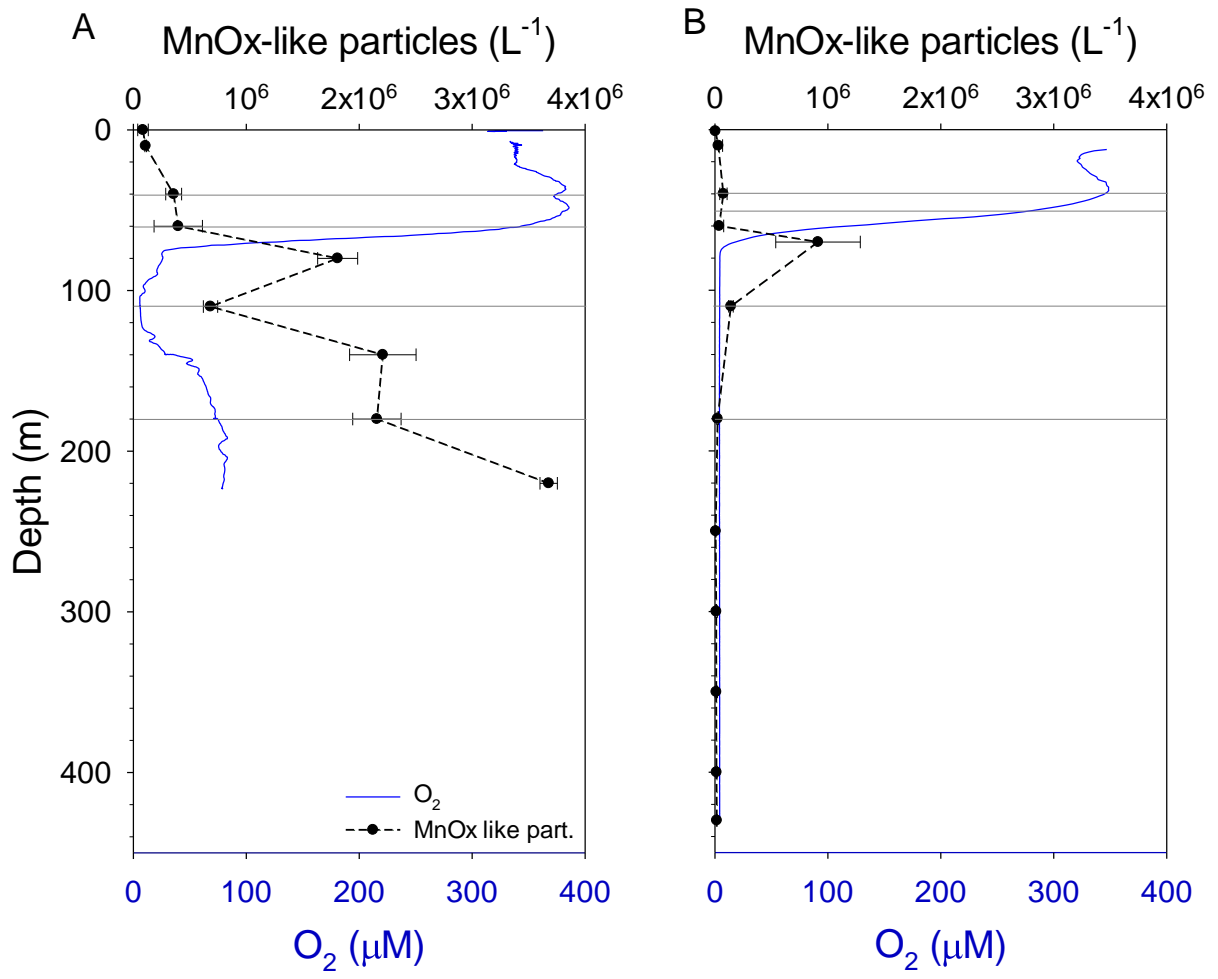


Fig. 4

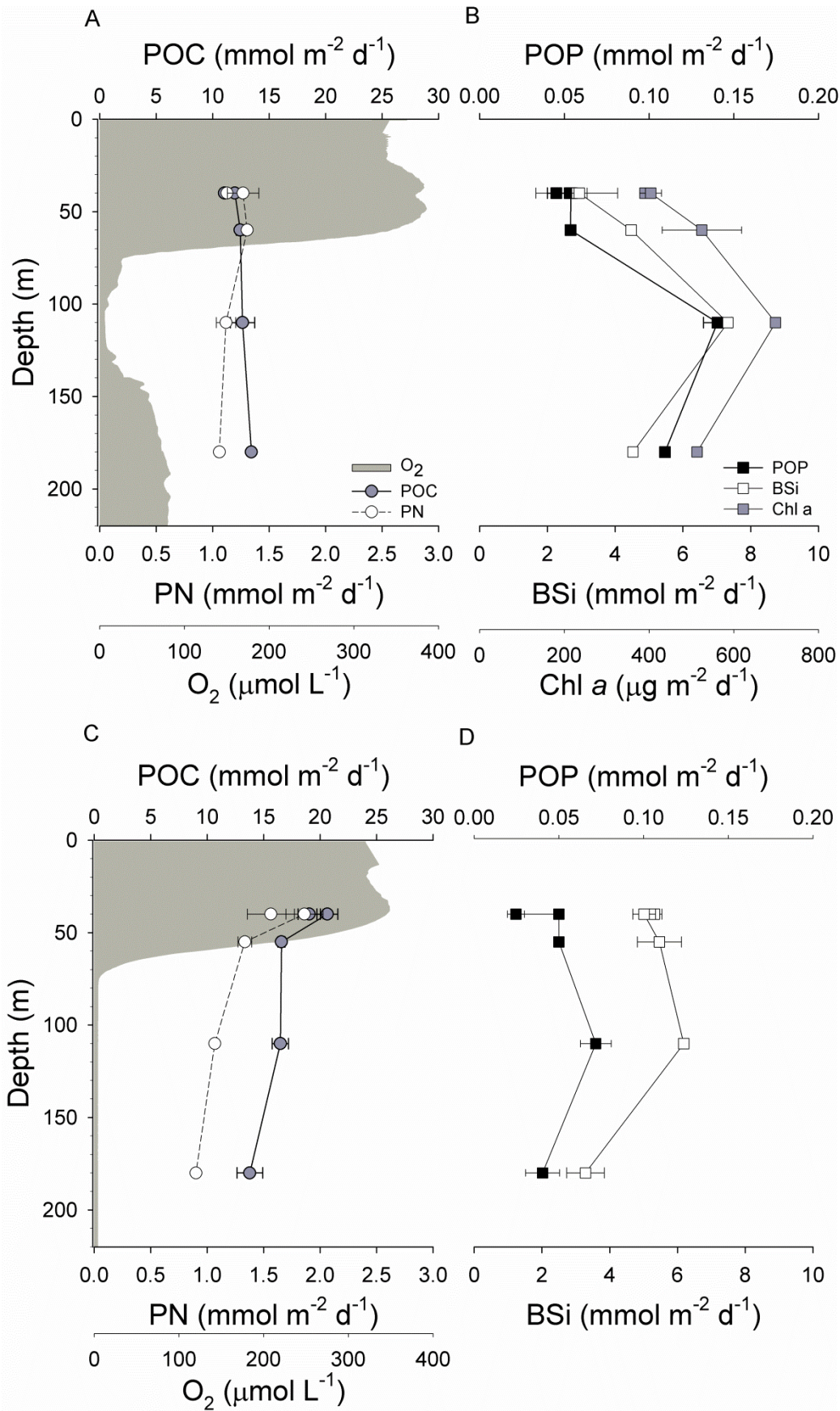


Fig. 5

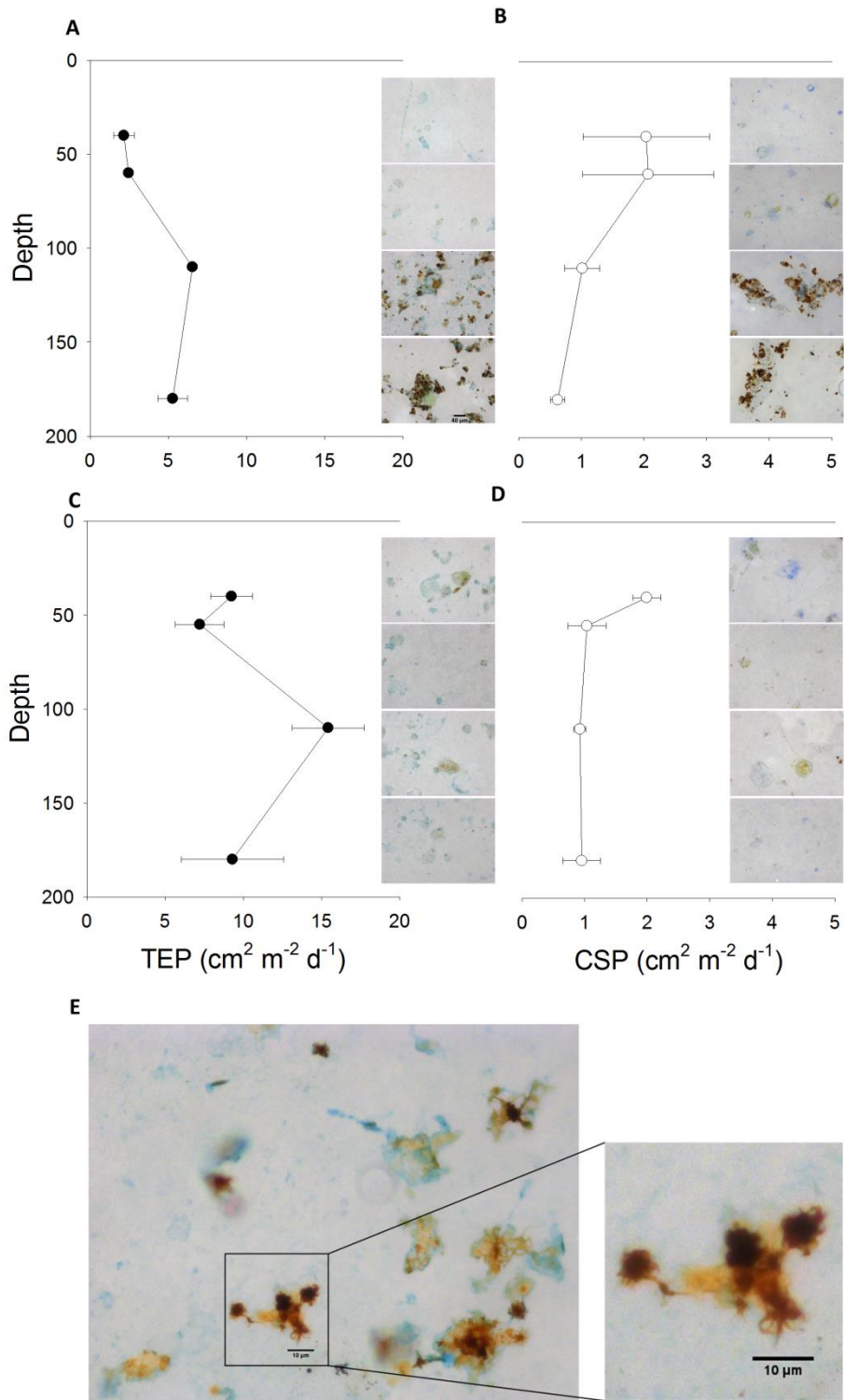


Fig. 6

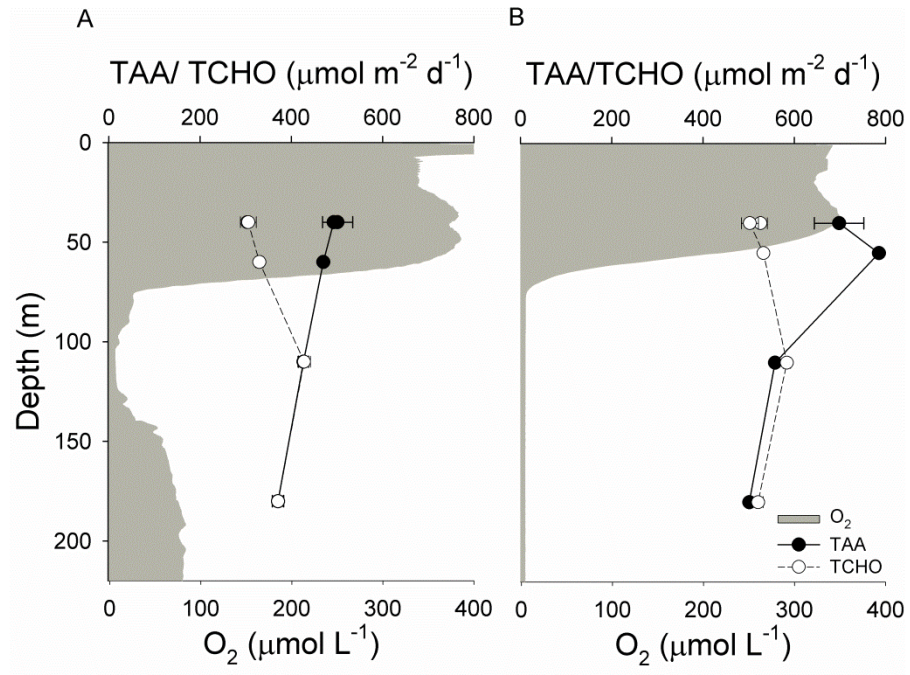


Fig. 7